

5-2018

A Zooarchaeological and Paleoclimate Analysis of Gadus Morhua Otoliths Recovered from the Sandwich South Site, Shetland Islands, United Kingdom

A. Douglas McNab

Bates College, amcnab@bates.edu

Follow this and additional works at: https://scarab.bates.edu/geology_theses

Recommended Citation

McNab, A. Douglas, "A Zooarchaeological and Paleoclimate Analysis of Gadus Morhua Otoliths Recovered from the Sandwich South Site, Shetland Islands, United Kingdom" (2018). *Standard Theses*. 43.

https://scarab.bates.edu/geology_theses/43

This Open Access is brought to you for free and open access by the Student Scholarship at SCARAB. It has been accepted for inclusion in Standard Theses by an authorized administrator of SCARAB. For more information, please contact batesscarab@bates.edu.

A Zooarchaeological and Paleoclimate Analysis of *Gadus*
Morhua Otoliths Recovered from the Sandwich South
Site, Shetland Islands, United Kingdom

A Senior Thesis

Presented to

The Faculty of the Department of Geology

Bates College

In partial fulfillment of the requirements for the

Degree of Bachelor of Arts

By

A. Douglas McNab

Lewiston, Maine

April 6, 2018

Table of Contents

Acknowledgements.....	1
Abstract.....	1
Introduction.....	2
The Shetland Islands	3
Norse Settlement of the Shetland Islands	4
The Sandwich South Site	5
Otolith Scleroclimatology	8
Stable Isotope Oceanography	10
Late Holocene Paleoclimate of the North Sea Region.....	12
Methods	13
Lab Methods	13
Results.....	19
Zooarchaeological results:	19
Geochemical results:	27
Discussion.....	35
Otolith Preservation and Taphonomic Bias	35
Otolith Geochronology Issues.....	36
Otolith Widths and Reconstructed Fish Lengths	38
Growth Rates	40
Paleoceanography of the Sandwich South Site.....	41
North Atlantic Paleotemperatures.....	44
Conclusions.....	46
Future Work.....	47
References.....	49

Table of Figures

Figure 1.1 Location map of Shetland Islands, Norway is to the East, Scotland to the Southwest, site is in blue box (Silverberg 2014).	2
Figure 1.2 Site Map of the Sandwick South Site (Bigelow 1985).	6
Figure 1.3 Cross sections of Midden Units 3 and 4, showing the stratigraphic complexity of the simpler midden units on the site (Bigelow 2017).	7
Figure 1.4, Thin sample of an otolith showing annual growth rings, scale bar=1mm (Hufthammer et al. 2010).	9
Figure 1.5, Isoscape of the North Sea Region, the Shetland Islands are in the top left corner of the map (Harwood et al. 2008).	11
Figure 1.6, Isoscape of $\delta^{18}\text{O}_w$ of surface waters in the Northwestern Atlantic Ocean (Legrande and Schmidt 2006).	12
Figure 2.1: Samples of otoliths from midden unit 2 with measuring bars.	13
Figure 2.2: Isomet low-speed sectioning saw with diamond blade.	14
Figure 2.3: Photograph of cross section of a sample otolith, with photographic settings highlighting growth rings.	16
Figure 2.4, Flowchart of otolith processing.	18
Figure 3.1: Sample H4-230/803-SU4, the smallest otolith found at the site.	20
Figure 3.2: Sample 2-225/828-1, the otolith on the far right is the largest otolith found on the site.	20
Figure 3.3: Histogram and scatterplot of fish lengths across the entire site, on scatterplot.	21
Figure 3.4: Scatter plot and Histogram of Fish Lengths for Midden Unit 1.	22
Figure 3.5: Scatter Plot and Histogram of Fish Lengths for Midden Unit 2.	23
Figure 3.6: Scatter Plot and Histogram of Fish Lengths for Midden Units 3 and 4.	24
Figure 3.7: Scatter Plot and Histogram of Fish Lengths for House Units 4 and 5.	25
Figure 3.8: Growth Rates of each Measured Otolith.	26
Figure 3.10: Radiocarbon Probability Curves for Midden Unit 1 Samples.	29
Figure 3.11: Radiocarbon Probability Curves for Midden Unit 2 Samples.	29
Figure 3.12: Radiocarbon Probability Curves for Midden Unit 3 Samples.	30
Figure 3.13: Radiocarbon Probability Curves for Midden Unit 4 Samples.	30

Figure 3.14: Radiocarbon Probability Curves for House Unit Samples.....	31
Figure 3.15 Oxygen isotope values for samples plotted against radiocarbon dates.....	32
Figure 3.16: Oxygen Isotope Data Histogram.....	33
Figure 3.17: Reconstructed temperatures plotted against the calibrated calendar year, archaeological phasing of samples by color of point, time periods of phases by color of box....	33
Figure 3.18: Histogram of Reconstructed Temperatures.....	34
Figure 4.1 Histogram of fish lengths from three sites in the North Sea from Van Neer et al. 2002 presented over the histogram of fish lengths from the Sandwich South site.....	40
Figure 4.2 Our growth rate data(top) with growth rate data from Van Neer et al. 2002(bottom), 3 archaeological sites and 2 modern regions with average growth rate data from the Sandwich South site, region VIId is immediately off the coast of the Netherlands, while region IVa is off the northwestern coast of Scotland.....	42
Figure 4.3 Isoscape from McMahon 2017 of ocean oxygen isotope values, with red representing more enriched and blue representing more depleted values. Note the yellow plume, the Gulf Stream, stretching up past England into the Arctic, and the dark blue fading to blue in the Baltic and North Seas.....	44

Table Of Tables

Table 3.1 Radiocarbon Ages with Error and Calibration applied.....	29
--	----

Acknowledgements

First, I'd like to thank my thesis advisors, Michael Retelle, Gerald Bigelow, and William Ambrose, for their patience with my endless questions and insecurities in taking on a project of this scope. Without their help, I never would have been able to find a project that fulfills my love of intersectionality between science and history, nor would I have had the resources to pursue it. I would also like to thank the Bates Student Research Fund, the Bates Geology Department, The Bates History Department, and the Bates Biology Department, for funding my testing materials, outside analysis, and attendance at conferences. In addition, I would like to thank Al Wanamaker, at Iowa State University, for providing me with stable isotope analyses of my sample otoliths, as well as Katherine Whitaker, at Northern Arizona University, for preparing my samples for radiocarbon dating. I would also like to thank my parents and my grandfather, who instilled in me a love of nature and science and taught me to be curious and think critically about the world around me. Finally, I would like to thank all my friends, and especially Colin Eimers, for dealing with my whinging about my data not working out, and the deadlines that were always immediately upon me. Special thanks to Daphne, for buoying my spirits frequently throughout the year.

Abstract

The Shetland Islands are an archipelago 240 km northeast of the northern tip of mainland Scotland and 360 km west of Bergen, Norway (Figure 1.1). The Gulf Stream, which flows from the Gulf of Mexico to the coast of Norway, passes along the western side of the Shetland Islands, leading to a warmer climate than would be predicted by their latitude. On the eastern side lay the colder waters of the North Sea, which also impact the climate of the islands. During the period in which the Sandwick South site was inhabited, 1100-1350 AD, paleoclimate reconstructions show a transition from a warmer period, the Medieval Climatic Optimum, to a distinctly cooler period, the Little Ice Age (Mann 2009). This transition has not been heavily studied in the Shetland Islands, as the acidic, non-arable soils of the Shetland environment makes many paleotemperature proxies difficult to reassemble. One paleotemperature record that can be used in the Shetland Islands is the otolith record, in which the $\delta^{18}\text{O}$ values of aragonite from inner ear bones of fish are utilized to reconstruct paleotemperature at the time the fish lived. These inner ear bones are collected from midden units within settlements. In addition to paleotemperature data, otoliths can also reveal information about the fishing methods of the inhabitants of the islands and ecological impact that the fishing had on the fish population.

Refining our knowledge of paleoclimate records can not only help to understand the potential future shifting of climate systems, but can also be a valuable tool in determining the effect that climate has on people living in the environment. Fish otoliths are an especially important source of information for a society heavily dependent on fishing for its livelihood, as they can provide a high resolution record throughout the inhabitation of a site.

Introduction

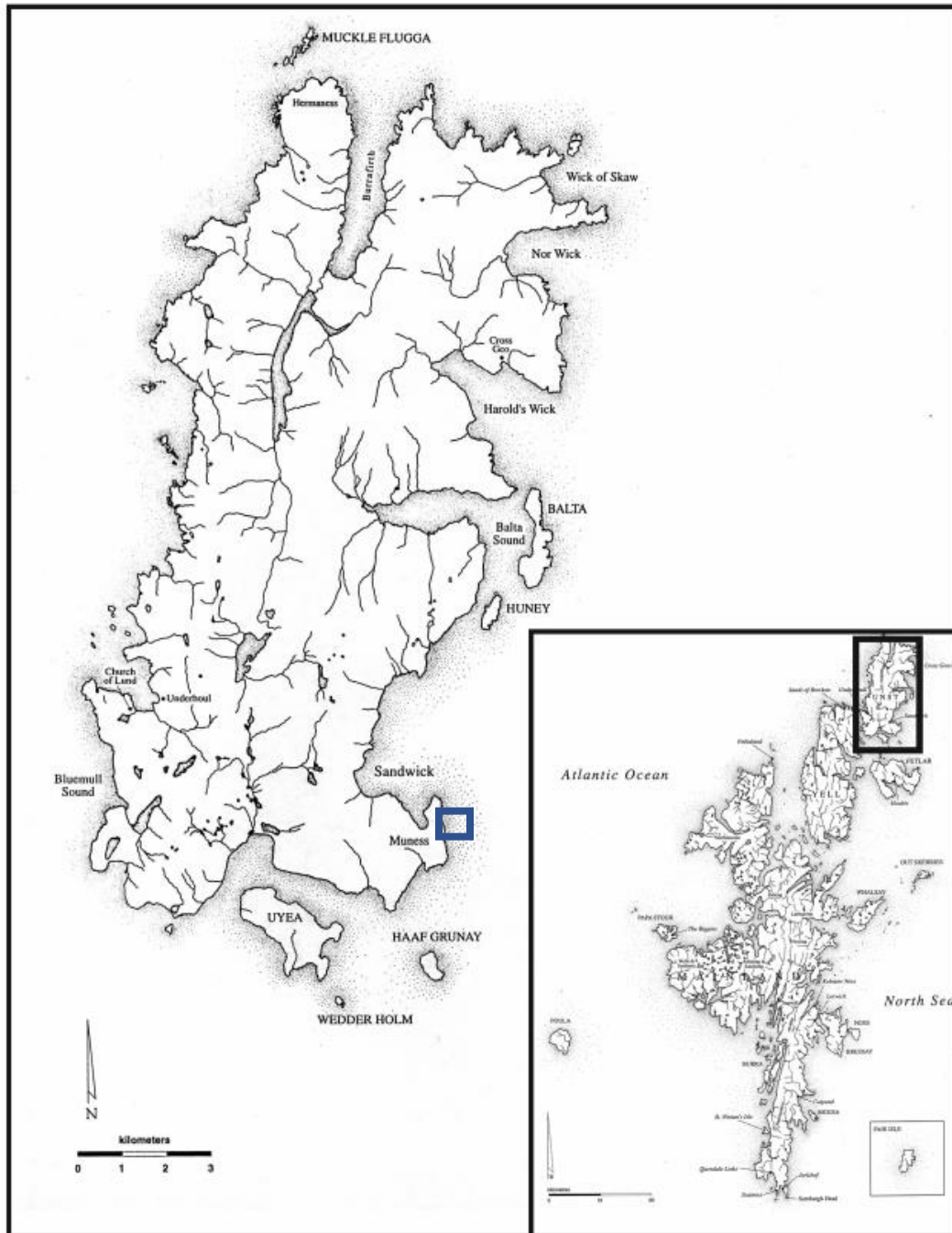


Figure 1.1 Location map of Shetland Islands, Norway is to the East, Scotland to the Southwest, site is in blue box (Silverberg 2014).

The Shetland Islands

The Shetland Islands are an archipelago that form part of the border between the North Sea and the Atlantic Ocean. They fall between -2 and 0 degrees E, and 59.85 and 60.87 degrees N. The island of Unst, on which the study is located, is the 3rd largest of the Shetland Islands (120.68 km²), and the furthest north of the main isles (Haswell-Smith 2004). The modern climate of the isles features long, cool winters, and short warm summers, both seasons being moderated by the effects of the nearby ocean currents, with the Gulf Stream in the east and the North Sea in the west. Modern August temperatures fall around 14.2°C, while modern February temperatures average 3.5°C (Lerwick Weather 2017). The wind and storminess of the islands is also notable, with the combination of a consistent source of water vapor and heavy winds coming across the North Sea leading to serious storms hitting the islands regularly. These conditions make Shetland a place in which people can live year-round comparatively easily but make it a difficult place to grow all but the hardiest crops. In addition to the climatic problems the bedrock geology also deeply affects the arability of the Shetland Islands. Most of Shetland is underlain by granitic rocks, which foster the growth of acidic peat bogs, and ultra-basic ophiolite, which is not a conducive place for peat-forming vegetation to grow. In addition, the peat bogs' high acidity tends to destroy bone and shell archaeological evidence. In some places however, shell sands have collected, creating a buffering basic environment in which preservation of shells, bone, and other acid-sensitive artefacts can take place (Bigelow 1989). These factors which force a dependence on fishing as a source of food, in addition to the rarity of shell and bone archaeological evidence in many parts of Shetland, lead to midden otolith evidence being an important paleoclimate proxy for the area. This study aims to use otolith evidence from the Sandwick South site to reconstruct the paleoclimate of the Shetland Islands from 1100-1350 AD,

as well as looking at age and growth rate changes in cod caught over that time period to determine possible anthropogenic forcings on the cod fisheries in the area.

Norse Settlement of the Shetland Islands

The first recorded Viking raids came to mainland Britain in the 8th and 9th centuries AD. Because of their strategically important position, the Shetland Islands were settled fairly early after the raids began (Bigelow 1989). Early settlement on Shetland was based on ease of access to the ocean, arable land, and steady peat supply for burning, however, there are very few sites where all three of these factors coexist, and as such later settlement had to make do with less favorable land (Bigelow 1989). These factors of limited arable soil, cool temperatures, frequent winds and storms, and short growing season limited the utility of agriculture as a major source of food for the Norse settlers of the Shetland Islands (Bigelow 1989). However, although the terrestrial resources of Shetland are lacking, the marine resources of the area are plentiful. Because of the confluence of the two different water masses, the North Sea and the Gulf Stream, the seas around Shetland are rich in nutrients, which provides for a robust ecosystem of fish, birds, seals, and shellfish (Bigelow 1989). As a seafaring people from a similarly marine rich environment, the Norse adopted a marine-based diet. This dependence on fishing continued to grow, and eventually as larger trade networks began to be established, Shetland was integrated into larger European trade. Fish would be exported, and luxury goods and grain would be imported to the islands (Bigelow 1985). This increased dependence on fishing is shown heavily in the preserved otoliths found at the Sandwick South site, enabling the current research into the paleoclimate and archaeological information stored within the otoliths.

The Sandwich South Site

The study site is located on the Southeast coast of the Island of Unst, the northernmost of the main Shetland Islands. It was rediscovered in the early 1900s, exposed by the draining of a nearby loch (Bigelow 1985). The site is in a bay with a sandy beach, and the site was partially buried by sand before its discovery (Bigelow 1985). A farmhouse and associated middens are present at the site, and have been notably well-preserved due to the high pH of the shell sand that covers the site (Bigelow 1985).. One source of archaeological material at the site is from within the house, where all periods of inhabitation are recorded, but the stratigraphy has been muddled by foot traffic. Outside the house, there are five midden deposits, three to the southwest of the house, two immediately adjacent to each other southeast of the house (Figure 1.2). Within these middens, four of them have otolith content, causing Midden Units one through four to be the primary target of our study. Within the site as a whole, three occupational phases have been identified by technological level and major physical changes to the site. Phase 1, the initial stage of settlement has been dated from 1100-1200 AD, and is marked in the midden deposits by a lack of pottery fragments, larger proportion of cod remains to pollock, large oval steatite vessels, as well as by characteristic dark, humic soils. (Bigelow 2017). Phase 2 midden deposits contain pottery fragments while the steatite vessels changed shape to generally square, suggesting the introduction of pottery around 1200 AD (Bigelow 2017). Phase 2 had two soil types, a pronounced sandblow event that did not have any bone or artifact evidence present within it, and a red to orange peat ash layer (Bigelow 2017). Imported goods also started to appear in greater numbers during phase 2, implying the beginning of trade networks including the Shetland Islands (Bigelow 2017). Phase 3 is characterized by the fewest bone artifacts, but a great increase in the number of calf bones found at the site (Bigelow 2017). In phase 3 deposits, pollock bones

greatly outnumber cod bones (Bigelow 2017) Phase 3 was a thick deposit across much of the site, and had dark soils grading to brown sand at the upper interface (Bigelow 2017). Midden

Units three and four, as well as samples from within the house, cover all three of the chronological phases of the site (Bigelow 2017). Midden Units one and two are only known to cover Phase 2, however there is some evidence that they could extend minorly into Phase 1 or 3 (Bigelow 2017). All stratigraphy in the site is complicated by crossbedding and uneven material deposition, as shown in figure 1.3.

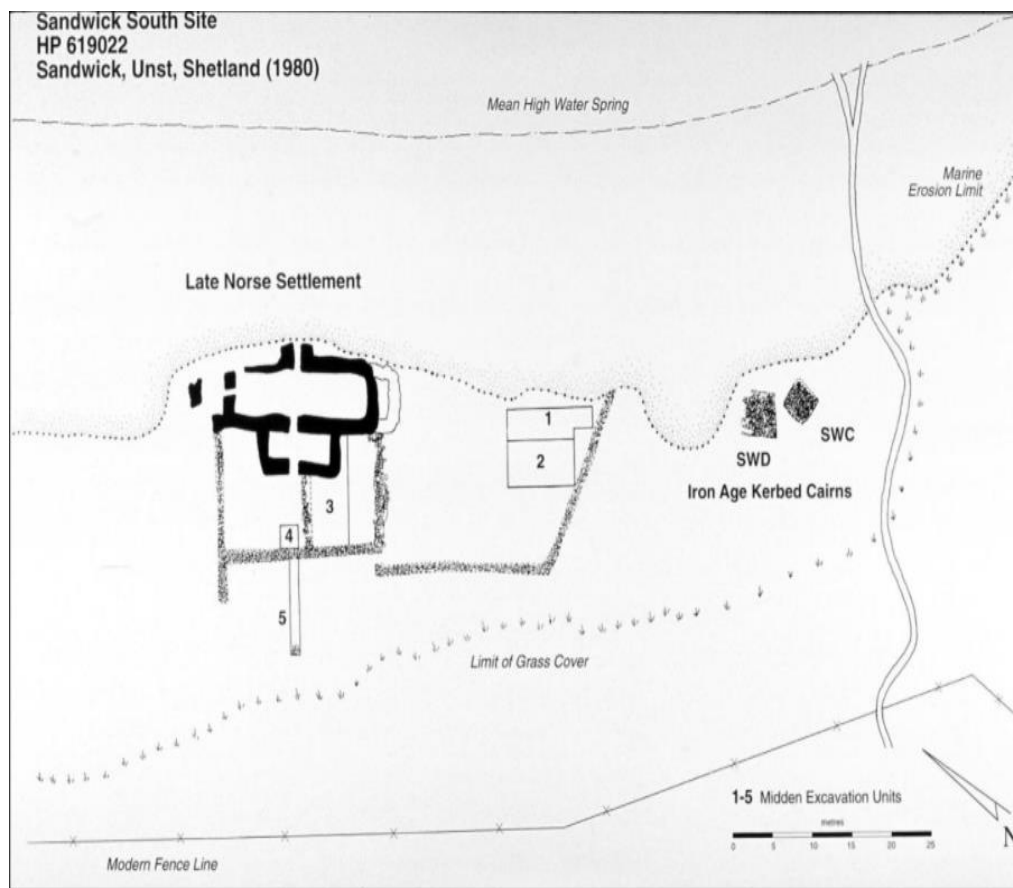


Figure 1.2 Site Map of the Sandwich South Site (Bigelow 1985)

Otolith Scleroclimatology

Otoliths are the inner-ear bones of any vertebrate and fulfill the same function of sensing gravity and movement in all vertebrate species. In fish, there is a well-documented linear relationship between the width of the otolith and the length of the fish from which it came (Van Neer et al. 2002). In addition to this, otoliths also have clearly defined annual accretions, with both winter and summer growth lines visible (Figure 1.4). When combined with the proportionality of the width of the otolith and the length of the fish, this annual growth signal can be converted into an annual growth rate over the life of the fish (Van Neer et al. 2002). These otolith growth features can be a valuable tool in looking at environmental conditions in which cod grow, as well as giving a historical comparison to the effects of modern fishing (Van Neer et al. 2002). Fish size can be used in archaeological analysis of fishing methods by looking at distribution of fish sizes across a period. If there are multiple concentrations of certain sizes across the sample, then there is the implication that these fish were being caught more often at those specific sizes. This kind of distribution can be caused by a variety of factors including different fisheries having different size cod, different fishing methods bringing in certain sizes of fish, and seasonal variation in cod size during their migrations past Shetland. Thus, a zooarchaeological analysis can give us information about the entire lifecycle of the cod, as well as potential interactions with human fishermen.

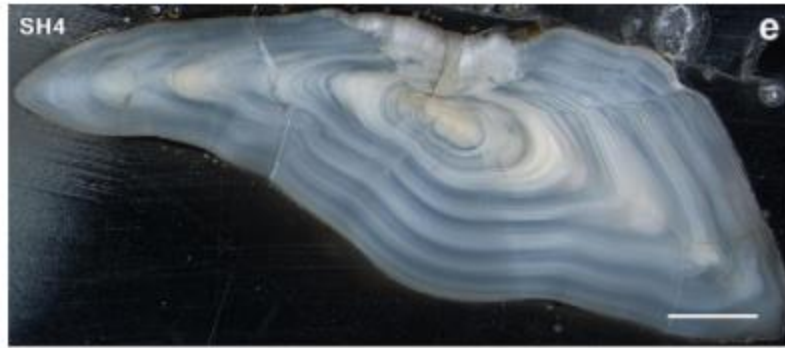


Figure 1.4, Thin sample of an otolith showing annual growth rings, scale bar=1mm (Hufthammer et al. 2010).

In addition to the zooarchaeological analysis of the otoliths, it is also possible to do geochemical analysis to determine both the age of the otolith and water temperatures in which the otolith formed. Otoliths are made of aragonite, an unstable form of CaCO_3 , and can therefore be analyzed both for radiocarbon dating, and $\delta^{18}\text{O}$ analysis, which can be extended into a paleotemperature record (Hufthammer et al. 2008). The radiogenic isotope of carbon, ^{14}C , has a half-life of $5,730 \pm 40$ years, and by looking at the proportion of ^{14}C in the sample over the proportion it had when it stopped incorporating new carbon into the structure, one can determine how many half-lives have been completed since carbon was being incorporated into the sample (ACS 2016). $\delta^{18}\text{O}$ analysis also works by looking at proportions of isotopes in nature, but instead of looking at radioactive atoms it focuses on the stable ^{18}O isotope (Sharp 2017). As oxygen is incorporated into the carbonate structure, it selectively takes up different isotopes at a rate dependent on the temperature that the water is at, as well as the isotopic composition of the water (Sharp 2017). In any given constant water sample, the higher the fraction of $^{18}\text{O}/^{16}\text{O}$, the lower the temperature of the water is, as lower temperatures are more conducive to the heavier isotope being incorporated into the carbonate (Sharp 2017). Different water masses have different isotopic values, so establishing a $\delta^{18}\text{O}_w$ for the area is essential.

Stable Isotope Oceanography

Modern $\delta^{18}\text{O}_w$ values for the North Sea have been documented by Harwood et al. in 2008, and indicate that within the North Sea, the waters near the Shetland Islands are the most enriched in $\delta^{18}\text{O}_w$, while the waters near the entrance to the Baltic Sea are the lowest. Many factors cause variance in $\delta^{18}\text{O}_w$, including river and stream inputs, cycling with bottom water, different currents interacting, and the balance of evaporation versus precipitation in the area (Sharp 2017). In the Shetland Islands, there is very little influence by stream and river input, as the landmass of the islands is too small to have a large watershed. Bottom water cycling also has a minimal impact on the waters off of the Shetland Islands, as most of the overturn in ocean circulation happens far from the Shetland Islands (Sharp 2017). The interaction of currents of varying composition is a major control on the isotopic composition of the waters off of Shetland, as two bodies with distinct $\delta^{18}\text{O}_w$ values interact quite close to the Shetland Islands. The North Sea, which is fed from the Baltic Sea as well as the Gulf Stream, grows more enriched in $\delta^{18}\text{O}_w$ as the water from the Gulf Stream starts to predominate over that of the very depleted Baltic Sea. This is shown in Figure 1.6, where the Gulf Stream waters with $\delta^{18}\text{O}_w$ values from 0.1-0.3‰ extend up to and past the British Isles to northern Norway (Figure 1.6). The Baltic Sea, on the other hand, is comparatively depleted, with $\delta^{18}\text{O}_w$ values down to -7.7‰ (Figure 1.6). Because of the great degree of current influence on the isotopic composition of the area, and the mixing that the currents cause, the relative evaporative or precipitation impacts on the $\delta^{18}\text{O}_w$ around the Shetland Islands are small.

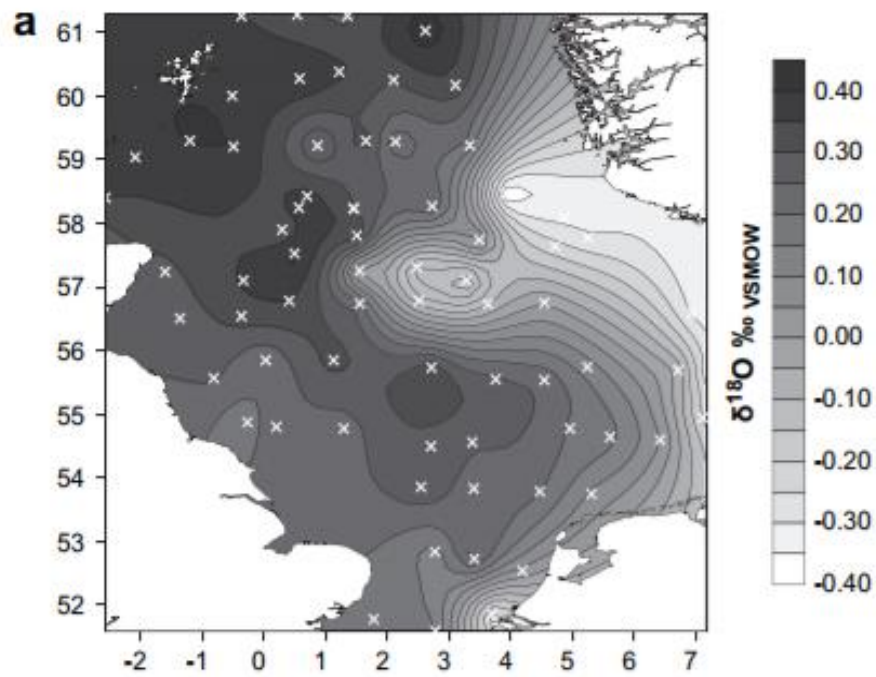


Figure 1.5, Isoscape of the North Sea Region, the Shetland Islands are in the top left corner of the map (Harwood et al. 2008).

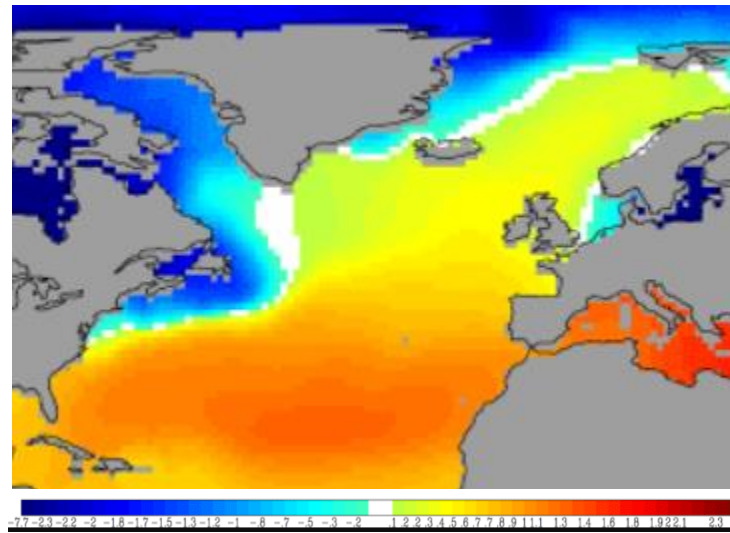


Figure 1.6, Isoscape of $\delta^{18}\text{O}_w$ of surface waters in the Northwestern Atlantic Ocean (Legrande and Schmidt 2006).

Late Holocene Paleoclimate of the North Sea Region

Many paleoclimate records exist in the area of the North Sea from a range of different proxies. The time period in which the Sandwick South site was inhabited is of particular interest to climate scientists, as there is a lot of debate over timing and character of the Medieval Warm Period which lasted from the 10th to 13th centuries (Mann 2009). The Medieval Warm Period (also known as the Medieval Climatic Anomaly). is heavily studied because although there are historical records that suggest that it existed (Lamb 1982), the geographical scope and magnitude of the warm period are unknown, prompting further study (Mann 2009, Bradley et al.2003). Büntgen et al. use a dendrochronological approach in the European Alps, and find temperatures increasing sharply from 1100-1200 AD from -1C to 0C, followed by a significant drop to below -1C, followed by a return to above 0C that then gradually declines until 1350 (Büntgen et al. 2005). The same trend is found in Büntgen's later 2010 work recorded in German Oaks (Büntgen et al. 2010). Sediment cores can also be used to reconstruct temperature through $\delta^{18}\text{O}$ analysis, using carbonate tests of foraminifera. Using foraminifera from Loch Sunart, an enclosed bay in the Orkney islands, Cage and Austin (2010). found very little bottom water temperature change during the period, with a dramatic drop and following warming in the temperature of the bottom water happening in the early 1200s, but no large scale trend being visible in the data. A combined proxy record, using ice core $\delta^{18}\text{O}$ data, tree ring data, and ice accumulation data across the entire northern hemisphere was made by Mann et al. in 2009, and shows a distinct cooling of the North Atlantic AMO region, followed by gradual warming until 1250AD, when the temperature decreases once more. A rise in temperatures happens from roughly 1290AD-1320AD, but a large drop in temperatures too place right as the Sandwick South site became uninhabited around 1350AD (Mann et al. 2002).

Methods

Lab Methods

Initially, the otoliths were separated into samples that could be analyzed, and those that could not based on the following criteria. First samples were sorted by whether or not the highest width on the otolith was preserved in the sample, as that is the location which needs to be measured for analysis of the otolith. Then, the passing samples were further sorted by whether there was evidence of corrosion on the edges of the sample, which showed in the form of dissolution features or chalkiness around the edges of the sample, which would influence the maximum width of the sample, leading to an underestimate of the length of the fish. Once this hand sorting was completed, the samples were laid out on a photography mat, with a ruler and the sample designation laid next to them. Photographs of the samples were taken with a Canon



Figure 2.1: Samples of otoliths from midden unit 2 with measuring bars

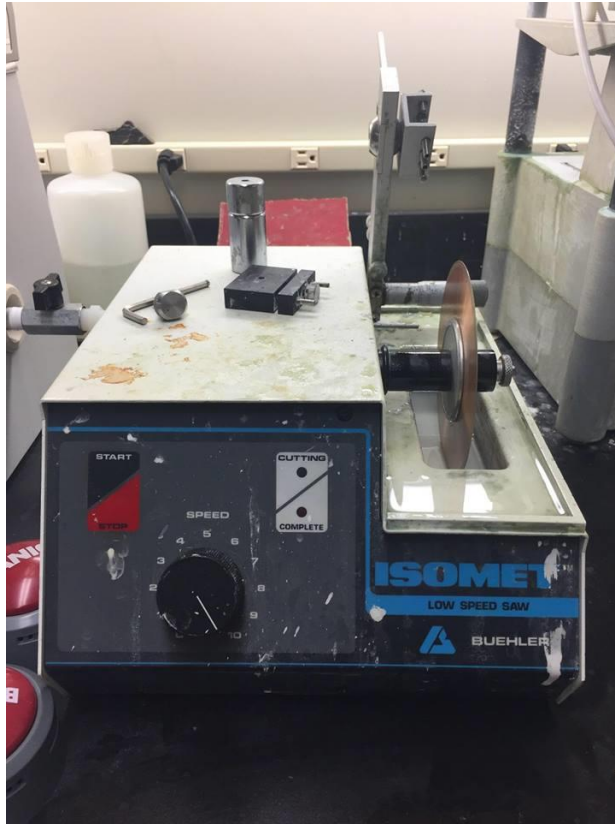


Figure 2.2: Isomet low-speed sectioning saw with diamond blade

EOS 3 camera, mounted on a rig that enabled top down photography. Samples were lit by floodlights on either side of the sample, to minimize shadows and increase the sharpness of the images. The digital photographs were then loaded into ImageJ a free software used for dendrochronology, where the scale was set to the same as a ruler in the background of the photographs, and then a line tool was used to measure the width of the otoliths (Figure 2.1).

Once the photographs are taken, the otoliths go through a more careful sample selection, with only the highest quality specimens with the minimum amount of weathering and the highest definition on the otolith ridges. These samples

form the core of the 30 strong sample set; other samples from different stratigraphic units were added to increase the chronological spread of the samples. With the fifteen highest quality samples, accounting for chronological spread, one end was broken off the otolith before the widest point on the otolith, and these fragments were set aside for further analysis. All samples were then marked with a sharpie along the widest point, to aid in sighting when cutting takes place. Then samples were set in Buehler resin, at a ratio of 4 parts resin to 1 part hardener in rubber sample cups. After setting for at least 6 hours, the resin was marked in line with the line marked on the otolith, and then placed into the chuck of an Isomet low-speed sectioning saw.

After the cutting was complete, the samples were taped together, and given labels with their Midden Unit, stratigraphic unit, and horizontal position.

The fragments that were set aside earlier from the best samples were subsequently broken up into two sections. One part was sent to the Stable Isotope Paleo Environment Research Group lab at Iowa State University for $\delta^{18}\text{O}$ analysis. Approximately 150 micrograms of otolith powder was vaporized, and analyzed with a ThermoFinnigan Delta Plus XL mass spectrometer with a Gasbench II, a CombiPal autosampler, a CosTech elemental analyzer, and a TC/EA using a ConFlo III interface (SIPERG 2017). The other part of the sample was sent to Northern Arizona University for sample preparation and then forwarded to the University of California Irvine for Radiocarbon dating through a low-resolution ^{14}C analysis. This analytical technique was different from traditional radiocarbon dating, in that it does not graphitized the samples prior to the spectrometry. In a traditional radiocarbon dating, the carbonates is burned to burn off the excess oxygen and form a pure carbon sample to be put through the spectrometer. However, when performing the low-resolution radiocarbon dating, one part by mass of carbonate was mixed with five parts by mass of iron and loaded into a cesium sputtering ion source(Bush et al. 2013). The equipment used in the lab was a National Electrostatics Corporation compact spectrometer, with a 0.5MV accelerator and an in-house modified ion source(Bush et al. 2013).

The samples that have been set in resin and cut were all then brought to the Bates College Imaging Center lab, where they were analyzed for growth rate and age analyses. To determine the age of the cod at death, the cross-section of the otolith was placed under a Nikon SMZ 1500 stereoscope, where an image was taken (Figure 2.3). Then, the alternating hyaline(dark). zones and opaque zones were counted. As each hyaline zone is a winter growth period, and each opaque zone is a summer growth period, each pair of the two is an annual

growth ring (Van Neer 2002). From there, the images were loaded into adobe photoshop, where a line tool was used to find the maximum width of the ring. This was then compared to a scale in a similar manner to the measurement of the full otoliths to find the real width of the growth

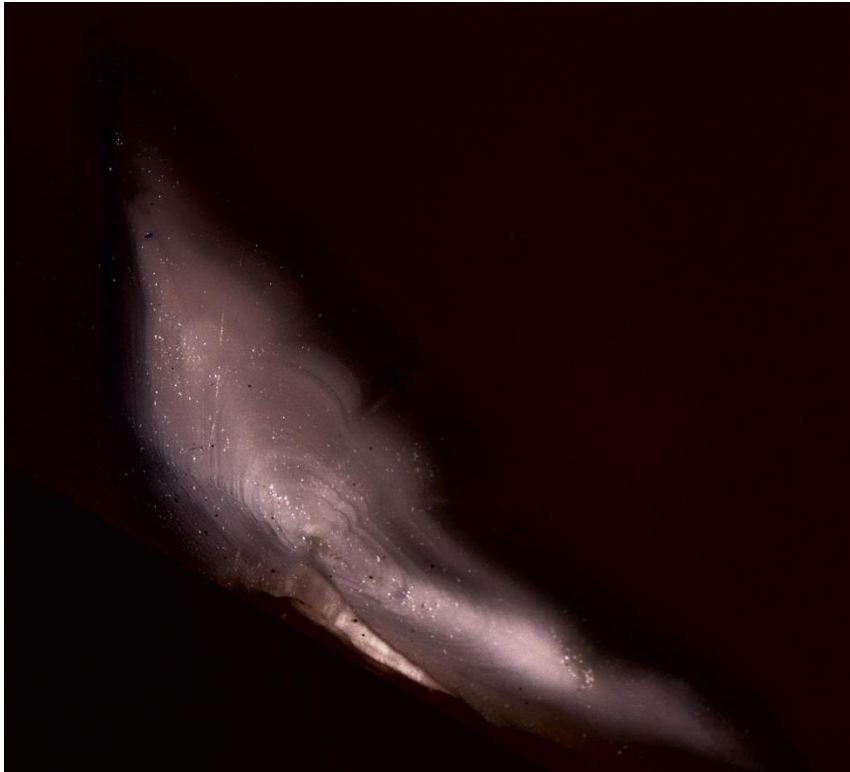


Figure 2.3: Photograph of cross section of a sample otolith, with photographic settings highlighting growth rings

rings.

Using the otolith widths from the photographic analysis, the lengths of the fish which they came from was reconstructed. When logarithmically corrected, the width of an otolith and the total length of the fish it came from have a linear relationship (Van Neer et al. 2002). The width of the otolith was taken at its widest point perpendicular to the sulcus, or central section that runs the length of the otolith. The total length of the fish is estimated from the tip of the snout to the end of the caudal fin. For this study, we used a natural log regression from Van Neer et al. 2002. In this formula, $\ln(FL) = a + b \cdot \ln(OW)$, otolith width is represented as OW, and input in millimeters, fish length, FL, is outputted in centimeters. The intercept, a, is 1.279, and the

slope, b , is 1.456 (Van Neer et al. 2002). The growth rate of the fish can be calculated using the same formula, but applied to the width of the growth rings rather than the total otolith width. The formula then becomes $\ln(FL_i) = a + b \cdot \ln(AW_i)$, where annuli width at age i is AW_i , and the fish length at age i is FL_i . By plotting these over the age of the cod, an annual change in length over the life of the cod is estimated.

The final step in the analysis of the otoliths was conversion of the geochemical data into usable paleoclimate data. The radiocarbon ages were calibrated using the Calib online function for marine reservoirs (Stuiver et al., 2017). This correction into calibrated or calendar years accounts for variable production of radiocarbon through time and spatial variability of the age of marine waters. For the ^{18}O analysis, the fractionation factor of aragonite was used in conjunction with the isotopic composition of the seawater in the area to determine a temperature of deposition for the aragonite in the otolith. The fractionation factor of aragonite used in this study was $1000 \ln \alpha = 16.75(\pm 1.33)(10^3 \text{ TK}^{-1}) - 33.49(\pm 0.307)$, which is derived from an Atlantic Cod otolith fractionation study done by Hoie et al. in 2004. The seawater $\delta^{18}\text{O}$ values were based on a North Sea $\delta^{18}\text{O}$ study done by Harwood et al (2008), who found $\delta^{18}\text{O}$ values of 0.35‰ in the area of the Shetland Islands. By dividing the known value of the $\delta^{18}\text{O}$ from the otoliths by the value of the seawater, a fractionation constant is obtained that was specifically related to the temperature of the water, as each temperature produces a unique fractionation constant.

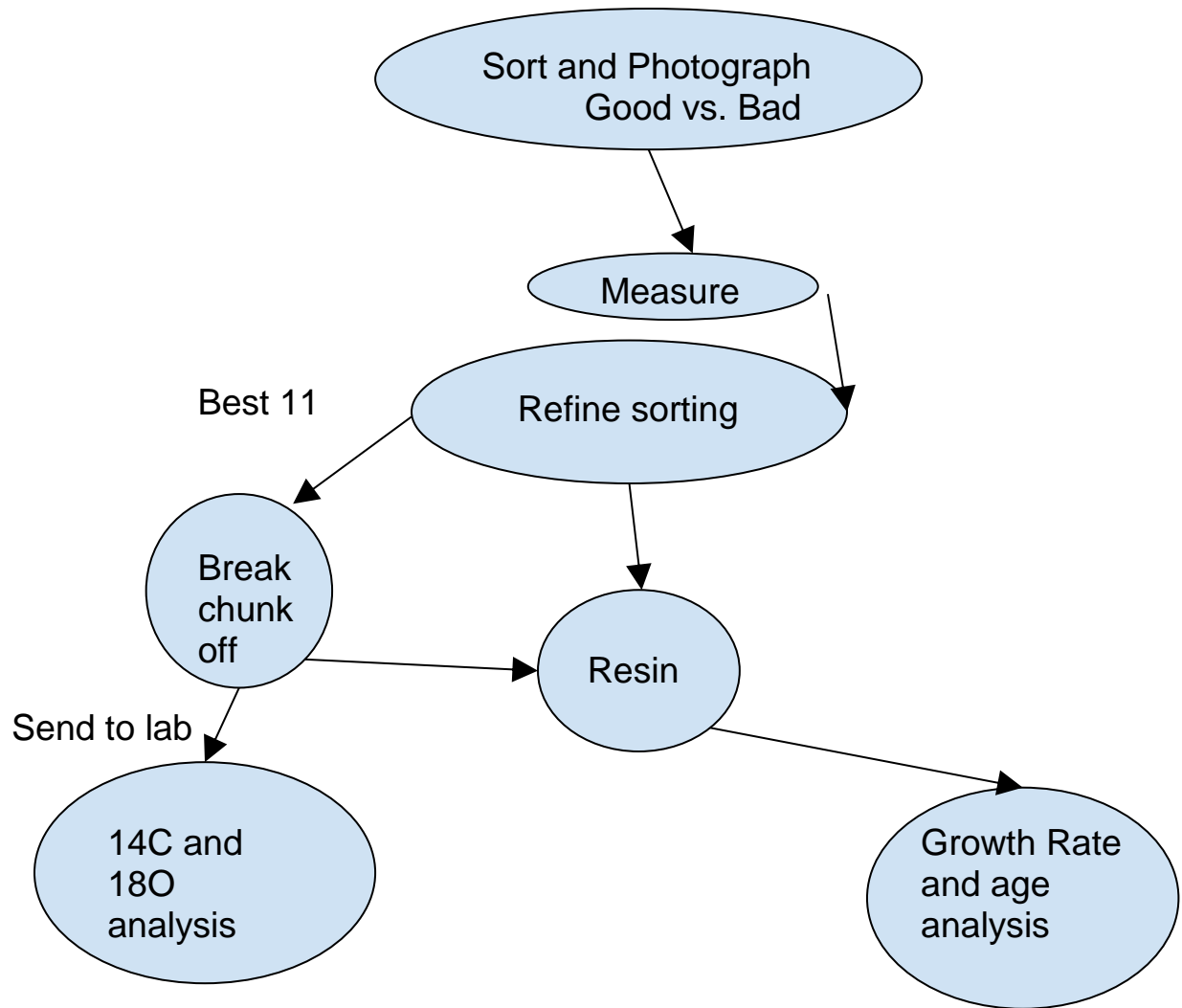


Figure 2.4, Flowchart of otolith processing

Results

Zooarchaeological results:

Otolith widths:

The smallest complete otolith from the Sandwick South Site is sample designation H4-230/803-SU4, which is 0.566 ± 0.001 cm collected from house unit 4 in the southern half of the house (Figure 3.1). The largest otolith excavated is sample designation 2-225/828-SU1-4, which is 1.123 ± 0.001 cm wide, collected from Midden Unit 2 in the southeast of the site. (Figure 3.2) Mean otolith width is 0.866 ± 0.001 cm, and the median otolith width is 0.878 ± 0.001 cm. When converted to fish length using the formula drawn from Van Neer et al. 2002, the fish lengths range from 32 ± 0.115 cm to 121.612 ± 0.158 cm, with the mean fish length being 83.270 ± 0.140 cm and the median fish length being 84.899 ± 0.141 cm. The distribution of all fish lengths has a unimodal distribution, with the most common size of cod at the site being between 80-100 cm long (Figure 3.3). Fish from 110-120 cm and 50-70 cm were 2nd and 3rd most common, respectively (Figure 3.3).

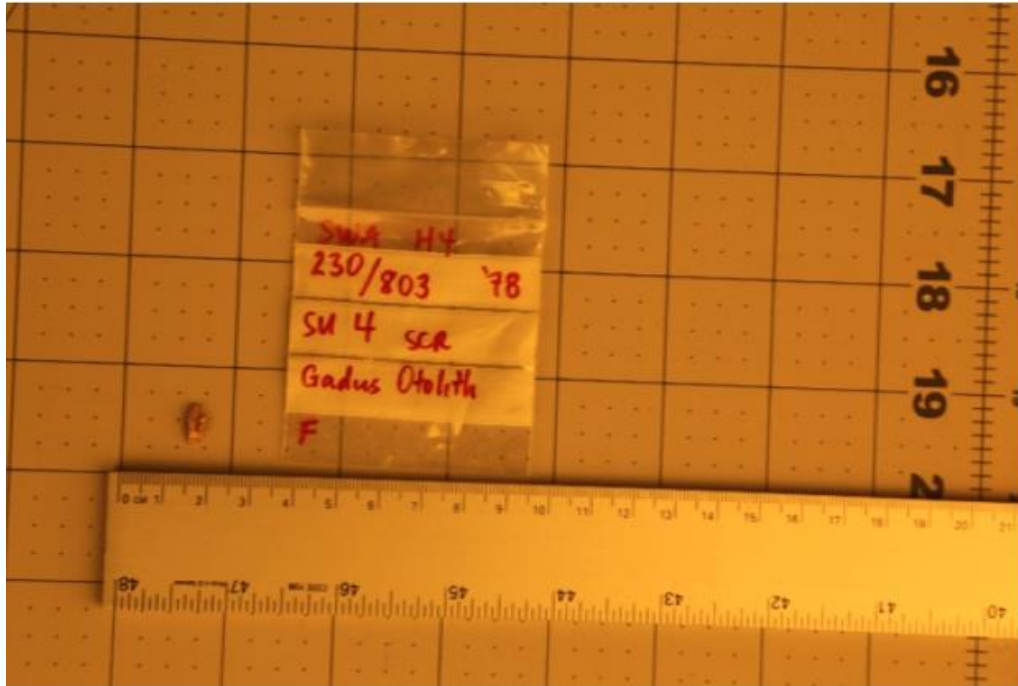
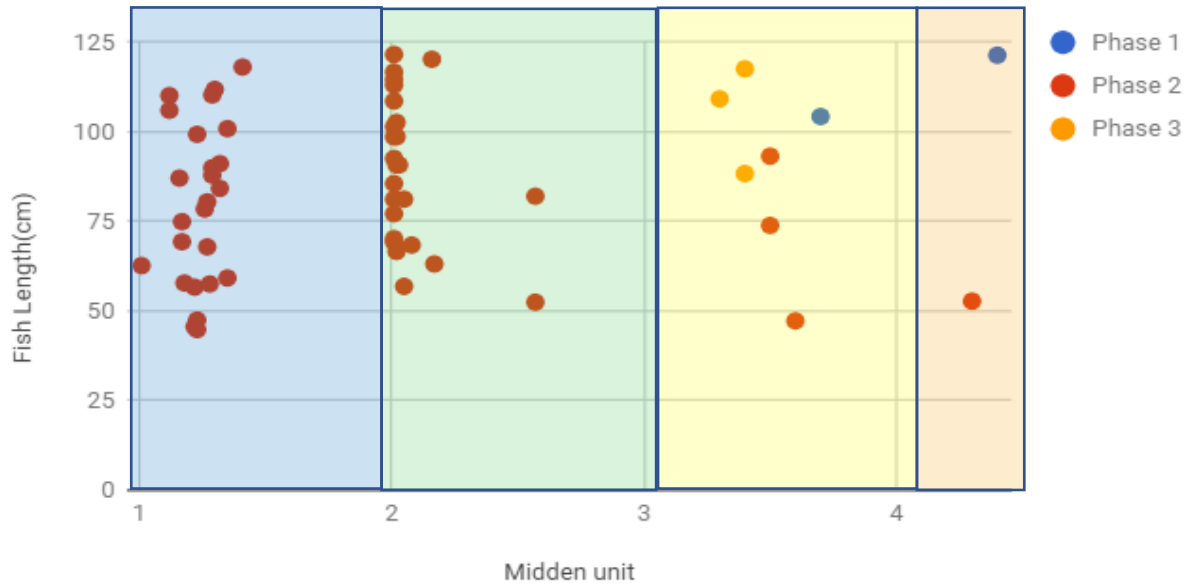


Figure 3.1: Sample H4-230/803-SU4, the smallest otolith found at the site



Figure 3.2: Sample 2-225/828-1, the otolith on the far right is the largest otolith found on the site

Scatterplot of Fish Lengths by Stratigraphic Unit and Midden Unit



Fish Lengths(whole site)

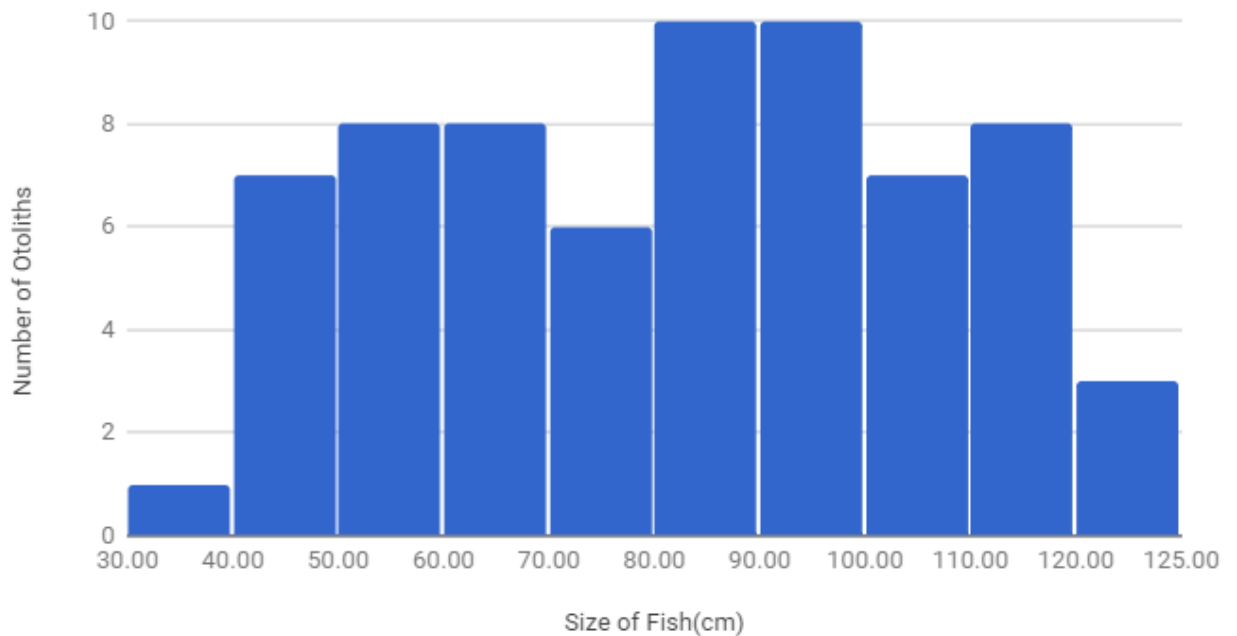
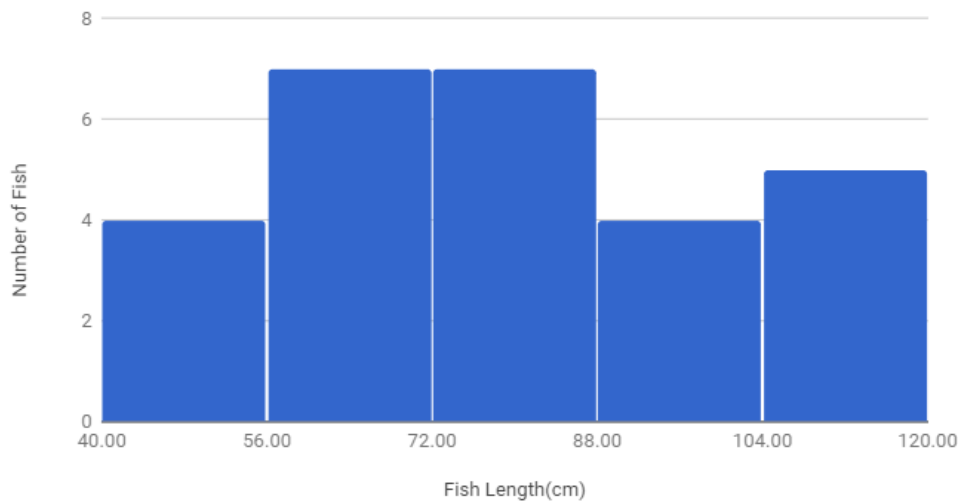


Figure 3.3: Histogram and scatterplot of fish lengths across the entire site, on scatterplot blue box is Midden Unit 1, green is Midden Unit 2, yellow is Midden Unit 3, and orange is Midden Unit 4

Within Midden Unit 1, the largest otolith measured is 1-227/830-SU 37-45, at 1.101 ± 0.001 cm wide, corresponding to a fish length of 118.134 ± 0.161 cm, while the smallest is 1-226/829-SU23 at 0.566 ± 0.001 cm, with a corresponding fish length of 44.863 ± 0.115 cm. Within this unit, average otolith width is 0.829 ± 0.001 cm, and average fish length is 78.004 ± 0.136 cm. For Midden Unit 1, the most common fish lengths were 50-60 cm and 80-90 cm, while the least common were 70-80 cm and 100-110 cm (Figure 3.4).

Fish Length in Midden Unit 1



Fish Length vs. Stratigraphic Unit

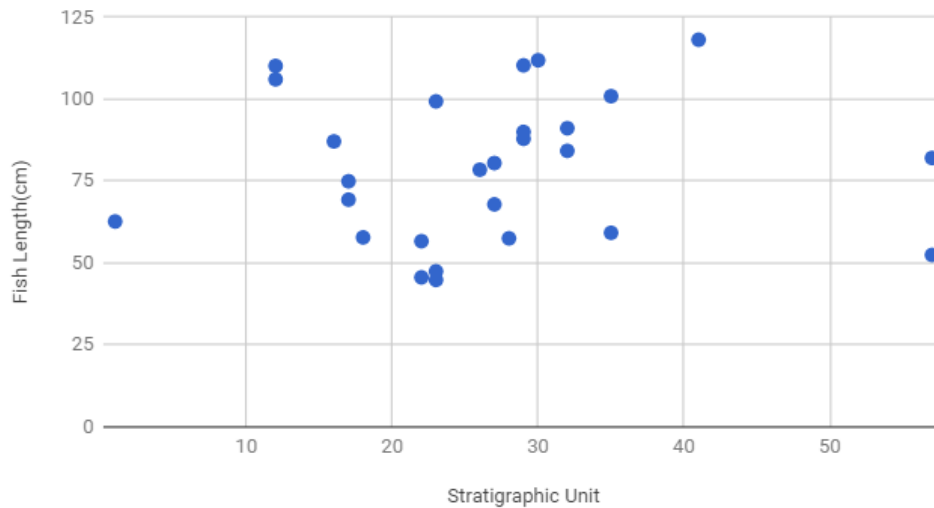
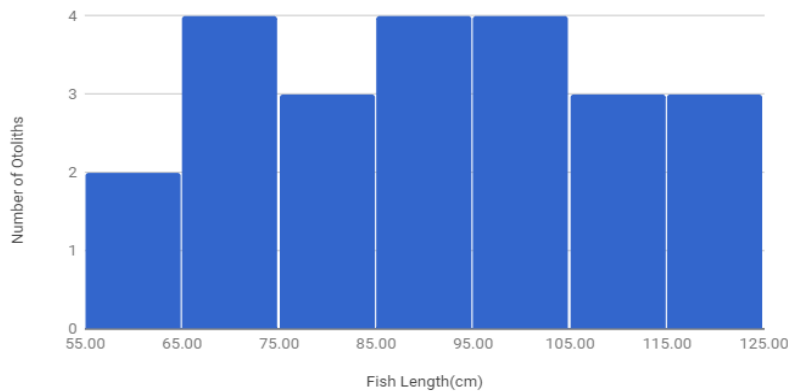


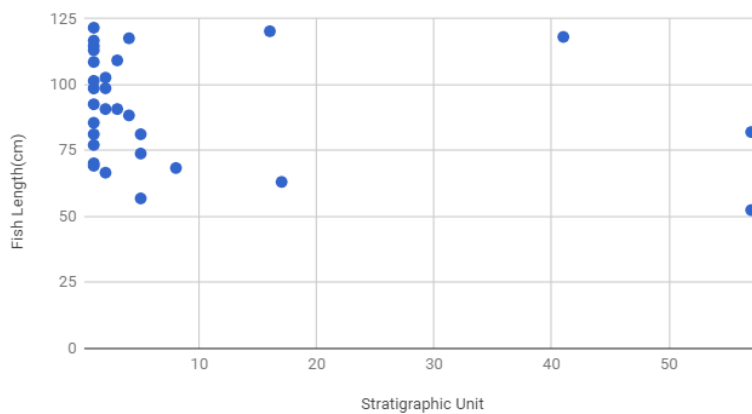
Figure 3.4: Scatter plot and Histogram of Fish Lengths for Midden Unit 1

Within Midden Unit 2, the largest otolith measured is 1-225/828-SU1-4, at 1.123 ± 0.001 cm, corresponding to a fish length of 121.612 ± 0.158 cm. The smallest otolith in Midden Unit 2 is 2-A8-SU17, at 0.716 ± 0.001 cm, corresponding to a fish length of 63.154 ± 1.26 cm. Within this unit, average otolith width is 0.915 ± 0.001 cm, and median otolith width is 0.919 ± 0.001 cm. Average fish length falls at 90.887 ± 0.146 cm, and median fish length is 90.781 ± 0.145 cm. Within Midden Unit 2, values were evenly spread across the size spectrum, with similar counts present in all 10cm groupings from 65-125cm (Figure 3.5). The smallest grouping, 55-65 cm, was the lowest count, but not only one count lower than the other groupings (Figure 3.5). Stratigraphic unit 1 had a large number of samples found in it.

Fish Length in Midden Unit 2



Fish Length vs. Stratigraphic Unit



Midden Units 3 and 4 are being combined for analysis due to proximity, low sample counts, and similar temporal scope. The largest otolith in Midden Unit 3 is 3-223/806-SU5, at 1.098 ± 0.001 cm, corresponding to a fish length of 117.620 ± 0.153 cm. The smallest otolith in Midden Unit 3 is 3-224/807-6, at 0.587 ± 0.001 cm, with a corresponding fish length of 47.266 ± 1.25 cm. The average otolith width for the combined midden units is 9.033 ± 0.001 cm, and the median otolith width is 9.358 ± 0.001 cm. The average fish length is 89.789 ± 0.144 cm, and the median fish length is 93.229 ± 0.148 cm. Because of the scarcity of samples from these two Midden Units, few conclusions can be drawn from histogram analysis, however the distribution skews towards larger fish, with $\frac{2}{3}$ of the fish lengths falling within the larger half of the distribution (Figure 3.6).

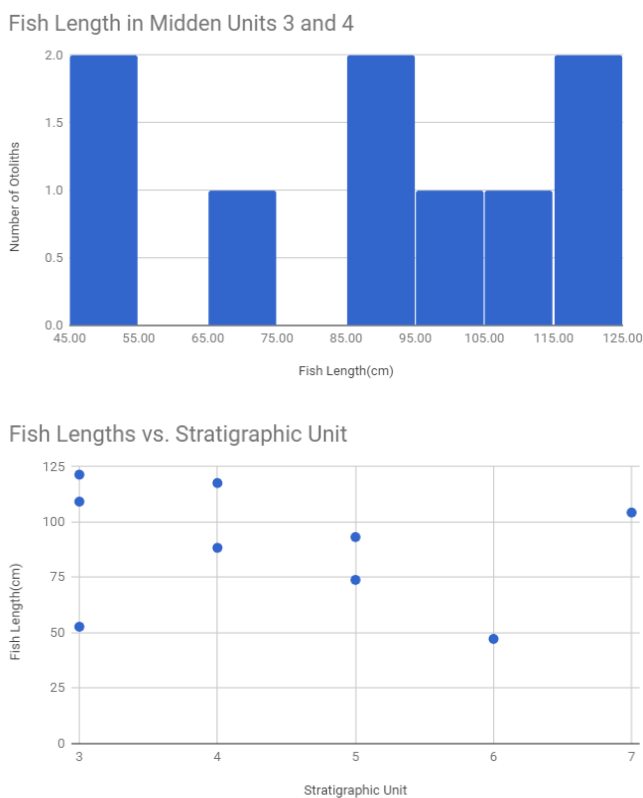
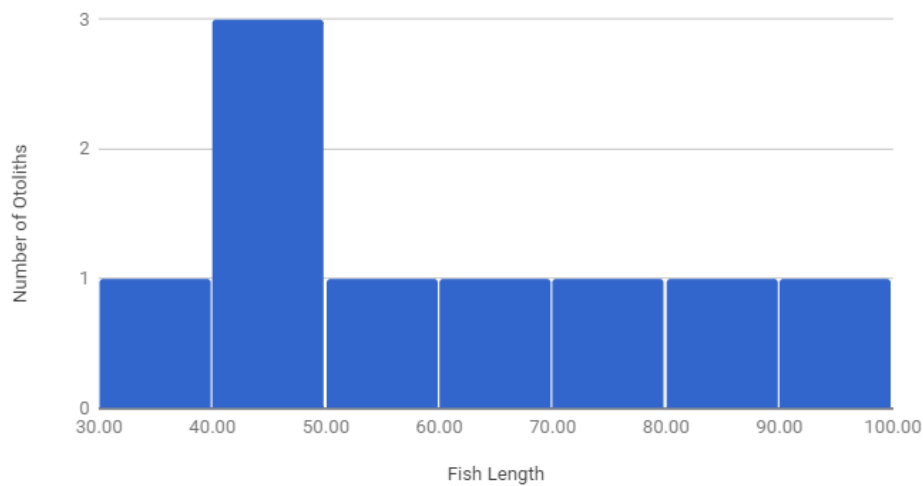


Figure 3.6: Scatter Plot and Histogram of Fish Lengths for Midden Units 3 and 4

Samples from the house units were by far the most scarce, with only 7 samples surviving in the quality necessary to measure. The largest of the surviving house otoliths is H5-230/807-7-2, at 0.977 ± 0.001 cm wide, corresponding to a fish length of 99.298 ± 0.029 cm. The smallest otolith in these units is H4-229/803-SU4/5-2, at 0.5547 ± 0.001 cm, corresponding to a fish length of 43.532 ± 0.011 cm. Most of the fish in these units fall between 45-55 cm in length (Figure 3.7).

Fish Length in House Units 4 and 5



Fish Lengths vs. Stratigraphic Unit

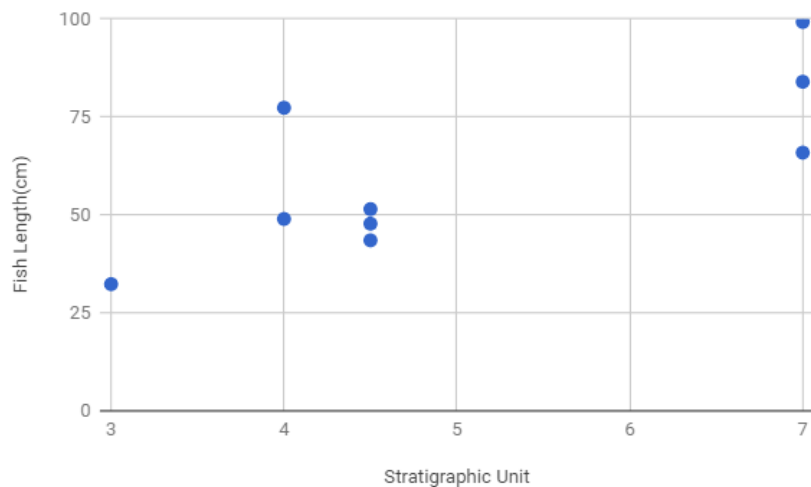


Figure 3.7: Scatter Plot and Histogram of Fish Lengths for House Units 4 and 5

Growth Rates:

Of the 38 samples set and cut, only 12 of these samples were usable for growth rate analysis due to low sample preservation. The degraded samples featured fractures, stains from chemical leaching, and structural issues caused by dissolution of the outer layers of the otolith. Most samples featured a small first annulus, followed by significant growth for 4-5 years, and then a significant lowering of the growth rate. Average size of the initial annuli is 9.190 ± 0.001 cm, while during the middle part of the cod's lives average growth rate is 16.083 ± 0.001 cm/yr. Post growth period, growth rates drop to an average of 7.73 ± 0.001 cm/yr. Average age of fish at time of catching drawn from measured otoliths is 5.8 years, with the mode being 6 years, no fish measured had more than 8 countable annuli (Figure 3.8).

Growth Rates of Measured Otoliths

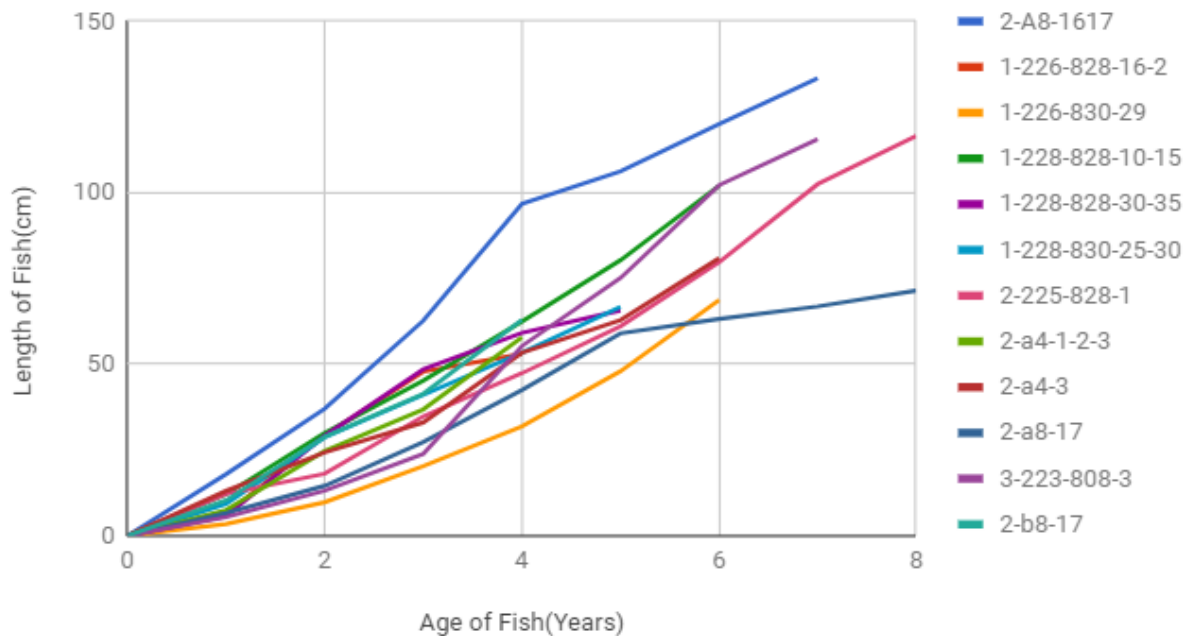


Figure 3.8: Growth Rates of each Measured Otolith

Geochemical results:

Radiocarbon Ages:

Fifteen samples were sent to the University of California Irvine to undergo radiocarbon dating. Radiocarbon ages range from 1680 ^{14}C years before present to 1080 ^{14}C years before present (Table 3.1). When calibrated using the Calib software, with a preset ΔR of 27 and an uncertainty of 6, the calibrated median probability ages span from 750-1330 AD. All but one of the values are between 1050-1330 AD when calibrated (Table 3.1).

Within Midden Unit 1, there were 4 samples sent for dating. Those samples returned calibrated ages of 1110 AD for SU17, 1120 AD for SU10-15, 1220 AD for SU26, and 1260 AD for SU30-35 (Figure 3.10). Three samples from Midden Unit 2 were sent, returning 1160 AD for SU5, 1220 AD for SU1, and 1260 AD for SU16/17 (Figure 3.11). Four samples from Midden Unit 3 were sent, returning 750 AD for SU6, 1050 AD for SU6, 1110 AD for SU3, and 1050 AD for SU6 (Figure 3.12). Two samples from Midden Unit 4 were sent, returning ages of 1010 AD for SU4, as well as 1100 AD for SU4 (Figure 3.13). Two samples from within the house were sent, with the sample from house unit 4 SU4 returning an age of 1330 AD, and the sample from house unit 5 SU7 returning an age of 1320 AD (Figure 3.14).

Sample Midden Unit	Sample stratigraphic unit	Sample area	mass of sample(mg)	¹⁴ C age	error	Calendar age	1SD	2SD
3	6	224/806	160	1680	90	746	655-838	573-955
4	4	218/298	106	1420	110	1006	893-1142	774-1243
3	6	224/807	19	1380	90	1054	966-1167	855-1252
4	4	218/298	67	1340	70	1098	1026-1174	953-1254
1	17	228/834	68	1330	70	1107	1033-1179	970-1263
3	3	223/808	116	1330	70	1107	1033-1179	970-1263
1	10-15	228/828	49	1320	70	1116	1041-1186	983-1267
3	7	224/807	180	1280	60	1151	1080-1217	1036-1272
2	5	B6	10	1270	70	1159	1080-1231	1031-1288
1	26	??	56	1210	60	1217	1170-1284	1074-1312
2	1	225/828	71	1200	80	1220	1154-1303	1047-1353
1	30-35	228/827	42	1160	90	1255	1168-1336	1073-1411
2	16/17	A8	52	1160	90	1255	1168-1336	1073-1411
H5	7	230/806	37	1090	100	1317	1249-1412	1127-1469
H4	4	230/803	12	1080	70	1330	1282-1396	1217-1442

Table 3. 1 Radiocarbon Ages with Error and Calibration applied

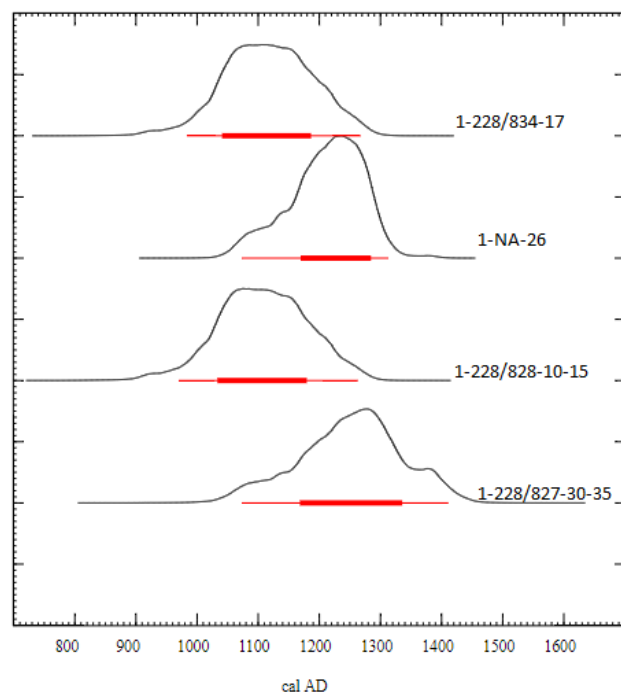


Figure 3.10: Radiocarbon Probability Curves for Midden Unit 1 Samples

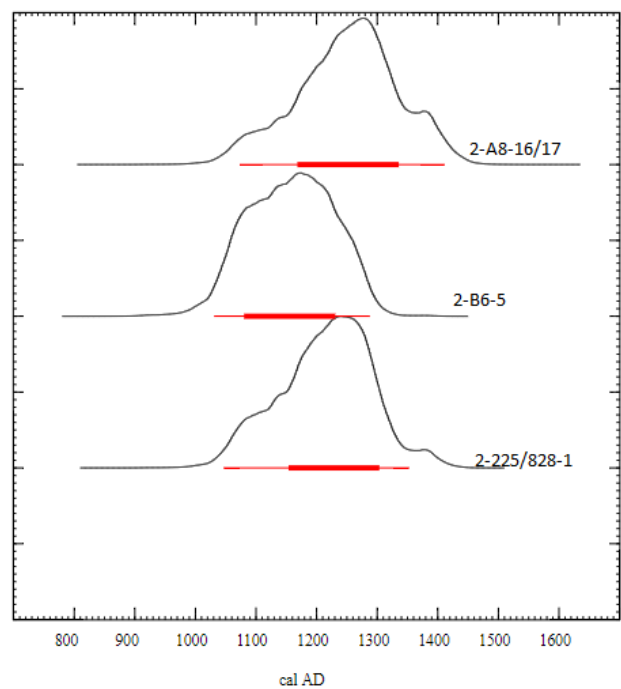


Figure 3.11: Radiocarbon Probability Curves for Midden Unit 2 Samples

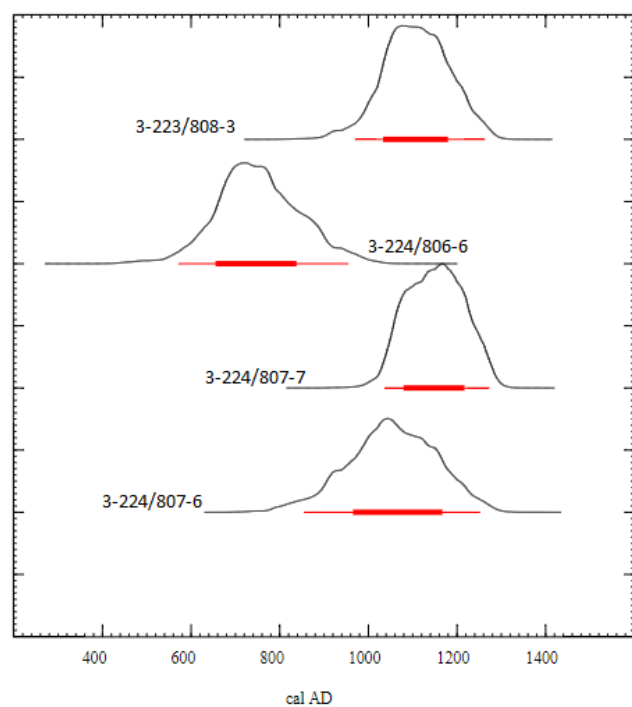


Figure 3.12: Radiocarbon Probability Curves for Midden Unit 3 Samples

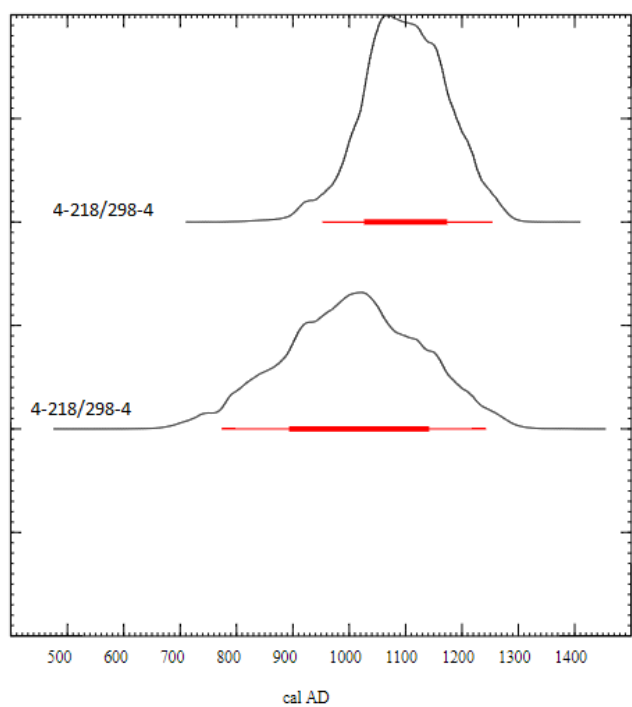


Figure 3.13: Radiocarbon Probability Curves for Midden Unit 4 Samples

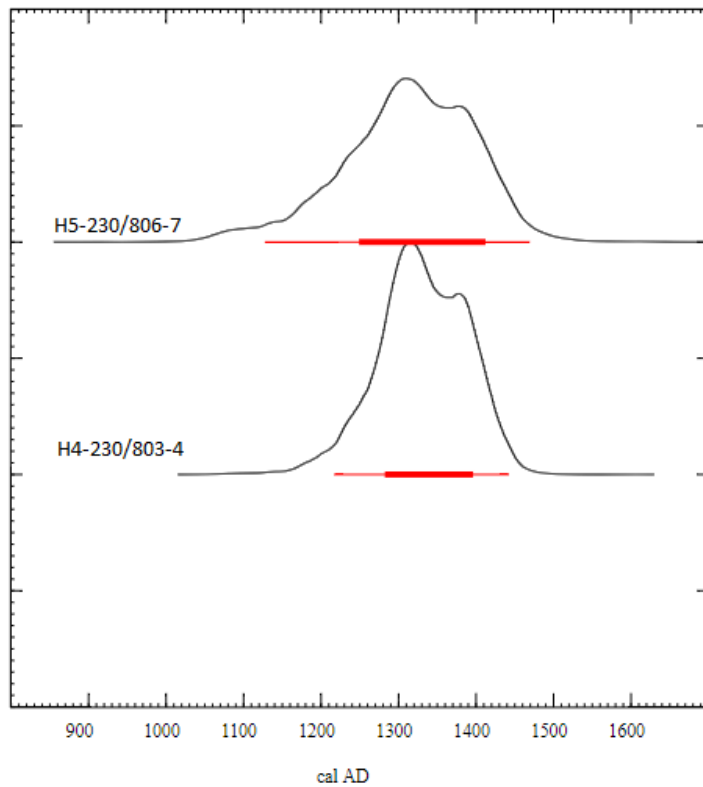


Figure 3.14: Radiocarbon Probability Curves for House Unit Samples

Oxygen Isotope analysis:

The same 15 otoliths samples for radiocarbon were also sampled for $\delta^{18}\text{O}$ values. $\delta^{18}\text{O}$ values range from $2.55 \pm 0.07\text{‰}$ for sample 1-NA-SU26 to $3.26 \pm 0.07\text{‰}$ for sample 1-228/828-10-15 (Figure 3.15). The average value for the samples is $2.95 \pm 0.07\text{‰}$, and the median is $2.91 \pm 0.07\text{‰}$. The distribution is bimodal, with values between 2.70‰ - 2.90‰ being the most common and 3.10‰ - 3.30‰ being second most common (Figure 3.16).

Ordered by calibrated radiocarbon age, samples from Midden Unit 1 had $\delta^{18}\text{O}$ values of $2.80 \pm 0.07\text{‰}$ for SU 17, $3.26 \pm 0.07\text{‰}$ for SU10-15, $2.55 \pm 0.07\text{‰}$ for SU26, and $2.89 \pm 0.07\text{‰}$ for SU30-35.(Figure 3.15) Samples from Midden Unit 2 had $\delta^{18}\text{O}$ values of $2.82 \pm 0.07\text{‰}$ for SU5, $2.91 \pm 0.07\text{‰}$ for SU1, $2.76 \pm 0.07\text{‰}$ for SU16/17.(Figure 3.15) Samples from Midden Unit 3 had $\delta^{18}\text{O}$ values of $2.82 \pm 0.07\text{‰}$ for the 750 AD SU6 sample, $2.71 \pm 0.07\text{‰}$ for the 1050 AD SU6

sample, $3.11 \pm 0.07\text{‰}$ for the SU3 sample, and $3.11 \pm 0.07\text{‰}$ for the SU7 sample.(Figure 3.15)

Midden Unit 4 samples had $\delta^{18}\text{O}$ of $3.18 \pm 0.07\text{‰}$ for the 1100 AD SU4 sample, and $3.18 \pm 0.07\text{‰}$ for the 1010 AD sample.(Figure 3.15) The house samples had $\delta^{18}\text{O}$ values of $3.09 \pm 0.07\text{‰}$ for H5-SU7, and $3.04 \pm 0.07\text{‰}$ for H4-SU4.(Figure 3.15)

Temperature Reconstruction:

Using the formula drawn from Thorrold et al. 1997, temperature was reconstructed using the Harwood et al. 2008 $\delta^{18}\text{O}_w$ data with a value of 0.35‰ . The average reconstructed temperature is $9.72 \pm 0.34^\circ\text{C}$, with the highest temperature calculated being $11.61 \pm 0.33^\circ\text{C}$ from the 1217 AD sample in Midden Unit 1 SU26, and the lowest temperature calculated being $8.24 \pm 0.29^\circ\text{C}$ from the 1116 AD sample in Midden Unit 1 SU10-15.(Figure 3.17) The median value for temperature is $9.90 \pm 0.33^\circ\text{C}$, and the distribution of temperatures is bimodal, with the $8.5\text{--}9^\circ\text{C}$ and $10\text{--}10.5^\circ\text{C}$ being the most common of the reconstructed temperatures (Figure 3.18).

Oxygen isotope ratios by radiocarbon date of sample

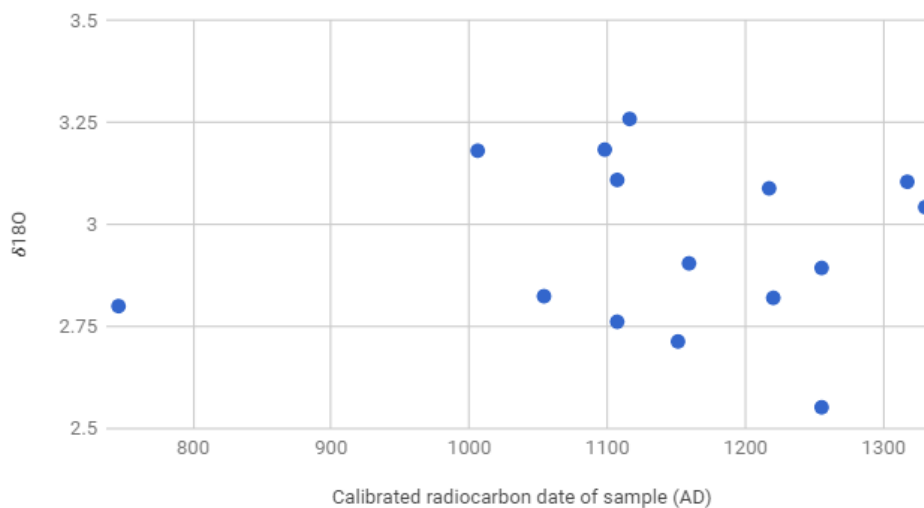


Figure 3.15 Oxygen isotope values for samples plotted against radiocarbon dates

$\delta^{18}O$ Histogram for all Samples

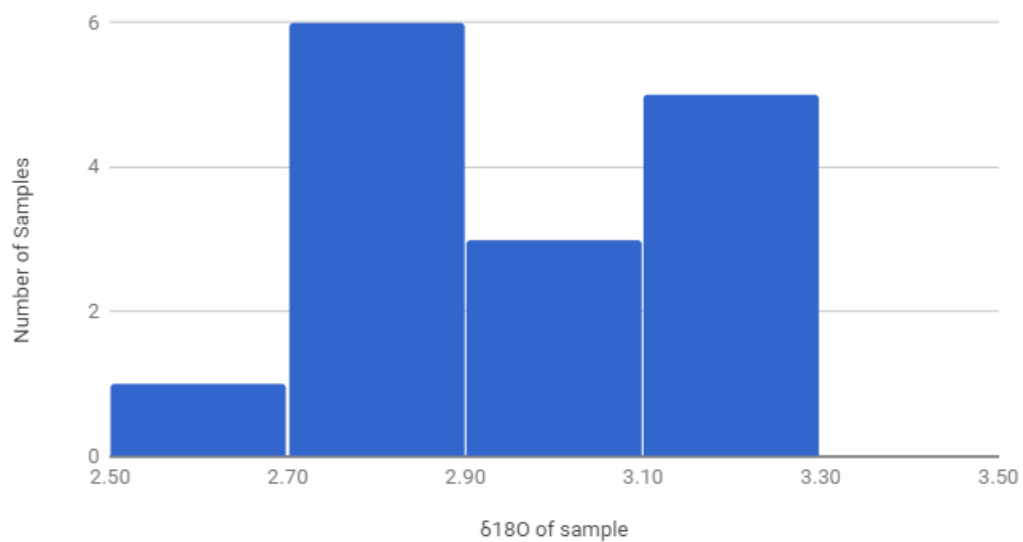


Figure 3.16: Oxygen Isotope Data Histogram

Temperatures Sorted by Radiocarbon Date and Archaeological Phase

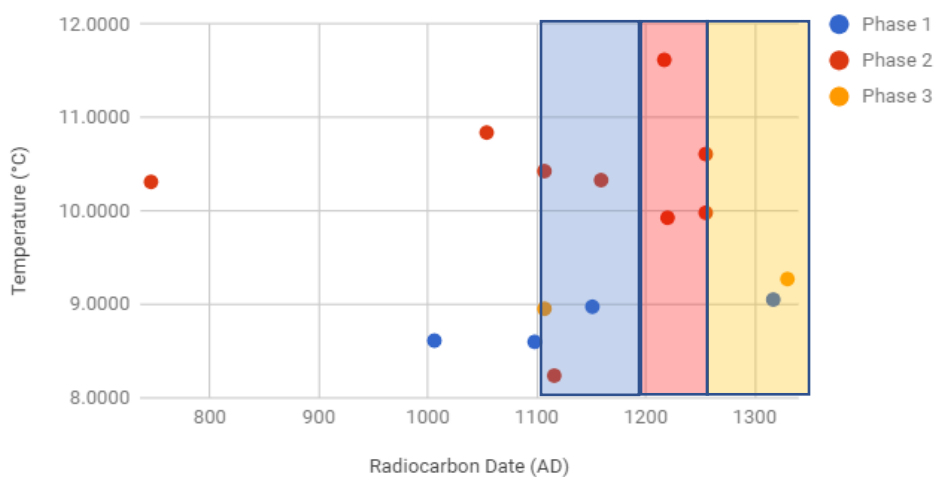


Figure 3.17: Reconstructed temperatures plotted against the calibrated calendar year, archaeological phasing of samples by color of point, time periods of phases by color of box

Reconstructed Temperature

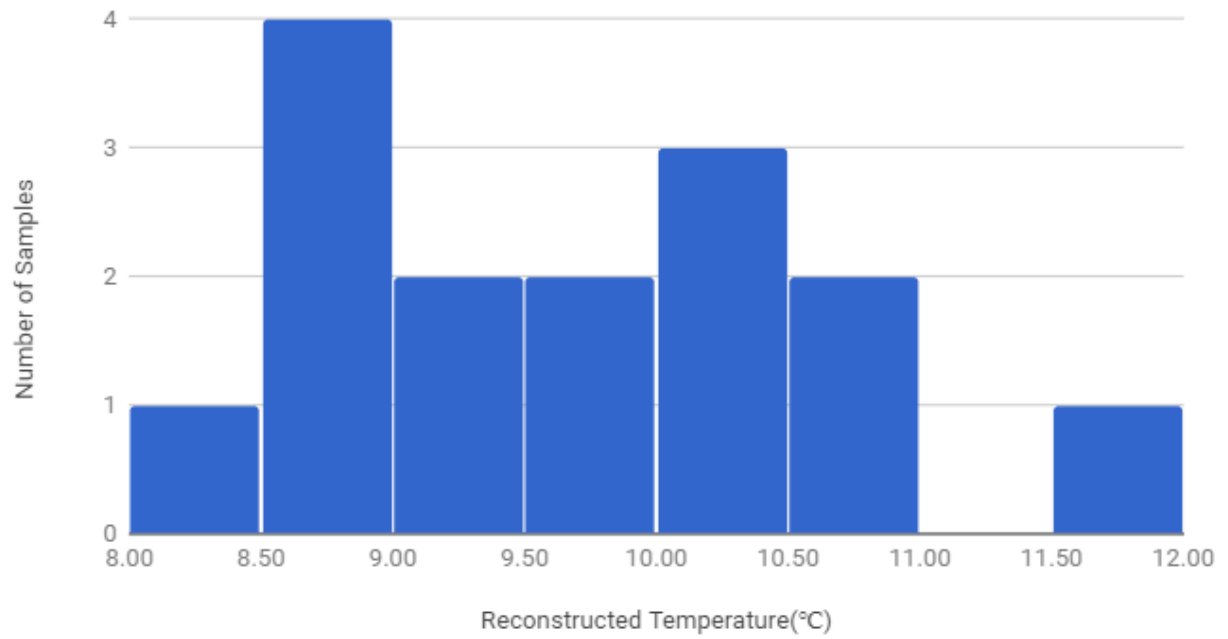


Figure 3.18: Histogram of Reconstructed Temperatures

Discussion

Otolith Preservation and Taphonomic Bias

Many of the otoliths collected from the site were only partial sections, with many missing $\frac{1}{2}$ to $\frac{3}{4}$ of their total volume of aragonite. Of the complete otoliths, many more were heavily corroded by environmental processes, whether by acid dissolution or the effects of water and salt on porous substances, these otoliths were extremely fragile, and often complete widths and lengths were not determinable. When complete, non-corroded otoliths were cut and sectioned, another type of degradation was occasionally present, staining caused by chemicals leaching in from outside the otolith obscured the growth rings and made them impossible to accurately read. In combination, these processes cause taphonomic bias, where groups of samples are preferentially rendered unusable for the analyses by natural processes that cause their breakdown. The otolith fragmentation was likely caused by pressure and impacts associated with their location in midden units, where they would have been disposed of without care for their preservation, had things thrown upon them, and where they would be walked upon. These specific processes would favor larger otoliths, as they are less fragile and therefore more likely to survive intact. The processes involving corrosion and staining are more dependent on the soil composition in which the otoliths are found, and as such vary widely by both midden and stratigraphic unit. In combination, this leads to large otoliths in basic soil conditions being the best preserved, while small otoliths in more acidic soil conditions are the least well preserved. This biases all fish size data towards larger fish, as well as potentially lowering the amount of data available from stratigraphic units with high acidity.

Otolith Geochronology

In Midden Unit 1, four sample otoliths were analyzed. In order by stratigraphic unit from bottom to top in the column, the ages from the otoliths sampled are 1168-1336AD, 1154-1303AD, 1033-1179AD, and 1041-1186AD. When compared to the age established by Bigelow (2017) for midden units of phase 2, 1200-1250AD, only 2 of the samples have standard deviations that fit within that range. Midden Unit 2 is much better for stratigraphic continuity, with the three samples in order of stratigraphic position being radiocarbon dated to 1168-1336AD, 1080-1231AD, and 1154-1303AD. Unlike Midden Unit 1, all three samples from this Midden Unit have standard deviations that overlap with the previously established period of use of Midden Unit 2, 1200-1250AD. Midden Unit 3 was also not stratigraphically continuous, with the 4 samples having radiocarbon ages of 1080-1217AD, 655-838AD, 966-1167AD, and 1033-1179AD when sorted by stratigraphic unit from bottom to top. In addition to the radiocarbon samples we analyzed, another study was done on a discreet sterile sandblow event represented in stratigraphic unit 6 (Figure 1.3), which used infra-red stimulated luminescence to date feldspars in the sand horizon (Kinnaird et al. 2015). The age of this sand horizon placed the sandblow at approximately 1250AD. This is 200 years after the later of the two radiocarbon dated otoliths recovered from the same unit (Kinnaird et al. 2015). In addition to these inconsistencies, there is a low age difference between samples from stratigraphic units 3 and 7 despite their different phases of occupation and stratigraphic distance from one another. Because of these factors, we are forced to conclude that all but one of the samples from Midden Unit 3 were affected by the ion exchange discussed earlier, making them unusable for accurate radiocarbon dating. The only sample usable from Midden Unit 3 is 1080-1217AD, which is one of the lowest of the standard deviations. Both samples from Midden Unit 4 were from stratigraphic unit 4, but they were

roughly 90 years apart, at 893-1142AD and 1026-1174AD. This difference, and the proximity to Midden Unit 3, suggests that Midden Unit 4 was also affected heavily by exchange with the environment, making these dates suspect. The house otoliths, which by stratigraphic unit should have been separated by a significant amount of time as parts of stratigraphic units 4 and 7, were instead only 10 years apart, being dated at 1330 AD for SU4 and 1320 for SU7. This evidence, in addition to the fact that the house had many renovations done and therefore likely has the most disturbed stratigraphy, invalidates these otoliths for being used in stratigraphic unit dating. Every single midden unit had at least one otolith that was not emplaced in the correct stratigraphic unit if the radiocarbon dates are correct. This forces the conclusion that using otoliths in this site for dating stratigraphic units is not a sound model. Instead, working within the previously dated phases and their corresponding stratigraphy (Bigelow 2017) is the best way to date the stratigraphic units.

The probable cause of these inconsistencies in the radiocarbon ages of the otoliths for Midden Units 1, 3 and 4 is exchange of carbonate ions with the environment around them. Otoliths are somewhat fragile and porous, and therefore likely to fracture and allow fluids into the matrix of the otolith. In addition, the soil in the area is primarily shell sands, which while aiding in the preservation of the otoliths over the 700 years since the abandonment also allowed exchange to happen. Shells, like otoliths, are composed of aragonite, and the frequent rains, sea spray, and possible groundwater influence moisten the ground in which the otoliths are sitting, enabling ion exchange between the shells in the sand and the otolith fragments (Douka et al. 2010). Carbonate ions from shells are likely to be older than the otoliths they are exchanging ions with, making the otoliths apparent age older than their actual age (Douka et al. 2010)

Otolith Widths and Reconstructed Fish Lengths

Overall, there does not seem to be a trend over time in the size of the otoliths found at Sandwich South, however, due to low sample size in Midden Units 3 and 4, as well as in the house units, the temporal coverage of the mass of our samples is limited to Midden Units 1 and 2, both of which are from phase 2 in the occupation of the site. In Midden Units 3 and 4, only 9 samples were preserved well enough to be measured, which when compared to the variety of otolith sizes within Midden Units 1 and 2 do not provide a firm picture of fish sizes over the period of occupation of the site. For the house otoliths, a combination of background information on renovations to the site and the radiocarbon ages proving unusable suggest that the stratigraphy in the house sections is heavily muddled, preventing a conclusion on the change of fish size over the occupation of the site.

Many studies have been done on fish size distributions at sites throughout the North Atlantic. Bigelow (1984) in his analysis of cod dentaries and premaxillae at the Sandwich South Site, discovered a bimodal distribution of fish sizes at the site in Midden Units 3 and 4, with modes at 45 cm and 88 cm. This bimodal distribution does not appear in our otolith data from primarily Midden Units 1 and 2. However, this bimodal distribution is found at many Norse sites across the North Atlantic, including those in Iceland, another locus for the cod trade. At Akurvík and Gjögur, two sites on the northwest coast of Iceland, Krivogorskaya et al. (2005) found a bimodal distribution of fish sizes with modes at 60 cm and 85 cm, windows attributed to different methods of fish preservation. This fish size distribution pattern is also present in Bessasstaðir, a fishing settlement just south of Reykjavik, where cod size modes were found at 45-60 cm and 90cm (Amarosi et al. 1992) Closer to Shetland, Van Neer et al. 2002 did studies on a variety of sites in the North Sea, and made size distributions for fish caught at each location

(Figure 4.1). Robert's Haven(1200-1400AD) and Raversijde(1425-1475AD) were both fishing settlements during the late-Medieval period, while Mechelen(1700-1800AD) only had access to cod by way of trade. While cod caught at Robert's Haven and Raversijde were in general smaller than those found in midden units in Sandwick South, the average fish size at Mechelen is slightly larger than that of Sandwick South.

The Shetland Islands during the late-Medieval period were a part of the cod trade to mainland Europe, but also featured subsistence fishing for the survival of the settlements (Bigelow 1985). The fish length evidence from the Sandwick South Site, reinforces the theory about trade and subsistence fishing being part of the lives of the Norse on the islands by having wider spread in fish length than any of the three sites studied by Van Neer et al., as well as similar spread to other Norse sites across the North Atlantic. Taphonomic issues may affect the relative proportions of large otoliths to smaller ones in the Sandwick South site, but the range of sizes is considerably larger at the Sandwick South site than at any of the Van Neer et al. sites, so the proportionality not being fully correct should not invalidate the trade and subsistence theory. A study done by James Barrett (1997) found evidence of fish trade happening in northern Scotland and the Orkney islands, areas that are likely to have been involved in the same trade routes as Shetland would have been. In addition, there are historical records of large scale fish trade happening in Caithness as early as 1349, which further validates the idea of a trade fishery in the northern North Sea (Barrett 1997).

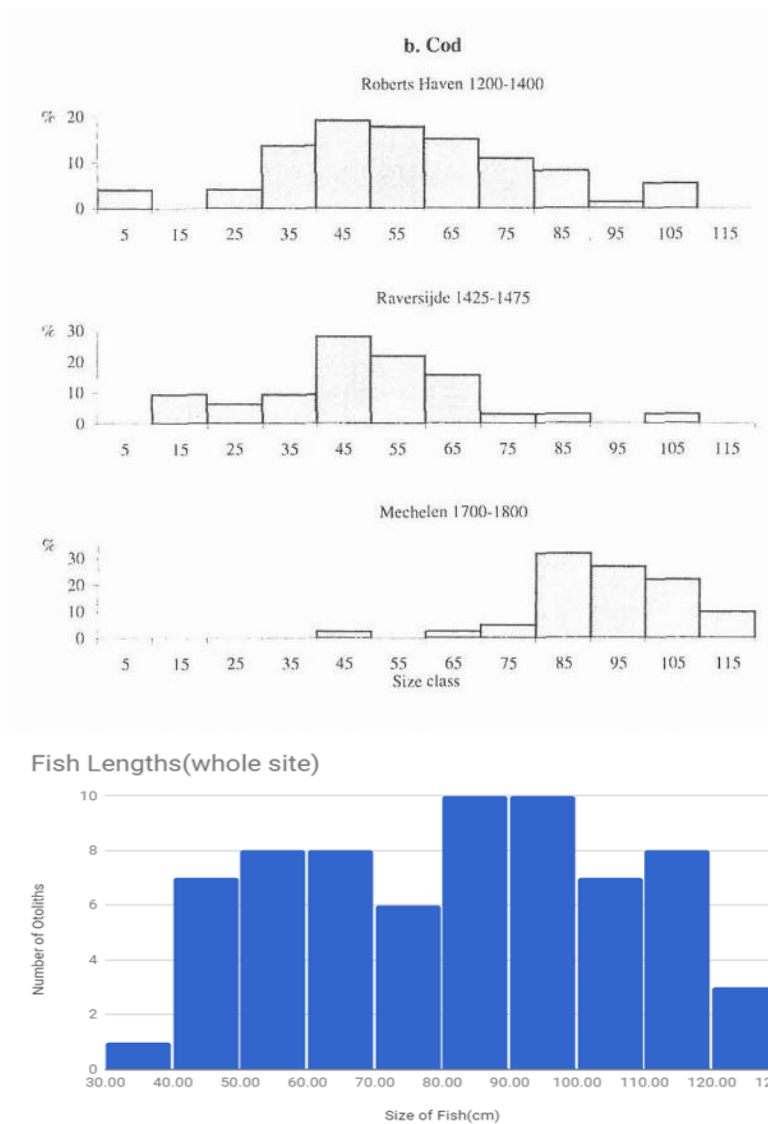


Figure 4.1 Histogram of fish lengths from three sites in the North Sea from Van Neer et al. 2002 presented over the histogram of fish lengths from the Sandwich South site

Growth Rates

Because of the rarity and poor sample preservation of samples from Midden Units 3 and 4, as well as from inside the house, only one sample from those units was analyzed for growth rate, meaning that almost all the growth rate data available is from Midden Units 1 and 2, both of which were active during phase 2. This prevents a study of growth rates over the full period of habitation of the site, as phases 1 and

3 are not represented. When compared to measured growth rates in archaeological and modern sites in the North Sea from Van Neer et al. 2002, the general pattern is slightly different.(Figure 4.2) Although both the Van Neer data and the data from Sandwick South have a steep early slope followed by a more shallow slope later in the life of the fish, the Van Neer data is a more classical ontogenic pattern with an exponential regression.

Paleoceanography of the Sandwick South Site

Because otolith paleotemperature reconstruction is based on both the temperature of the water and the isotopic content of the water, any approach to determining the paleoclimate of the area must account for both variables. Following the approach of Surge and Barrett (2012), which assumed constant $^{18}\text{O}/^{16}\text{O}$ ratios since the period which the study focused on, 900-1200AD, this study used the modern $^{18}\text{O}/^{16}\text{O}$ ratio of the seawater around Shetland from Harwood et al. (2008) as the basis of temperature reconstructions. This approach ignores a variety of influences on $^{18}\text{O}/^{16}\text{O}$ ratios that we know take place in the currents on the border between the North Atlantic and the North Sea. A dominant force in the water temperature and $^{18}\text{O}/^{16}\text{O}$ ratio of the water

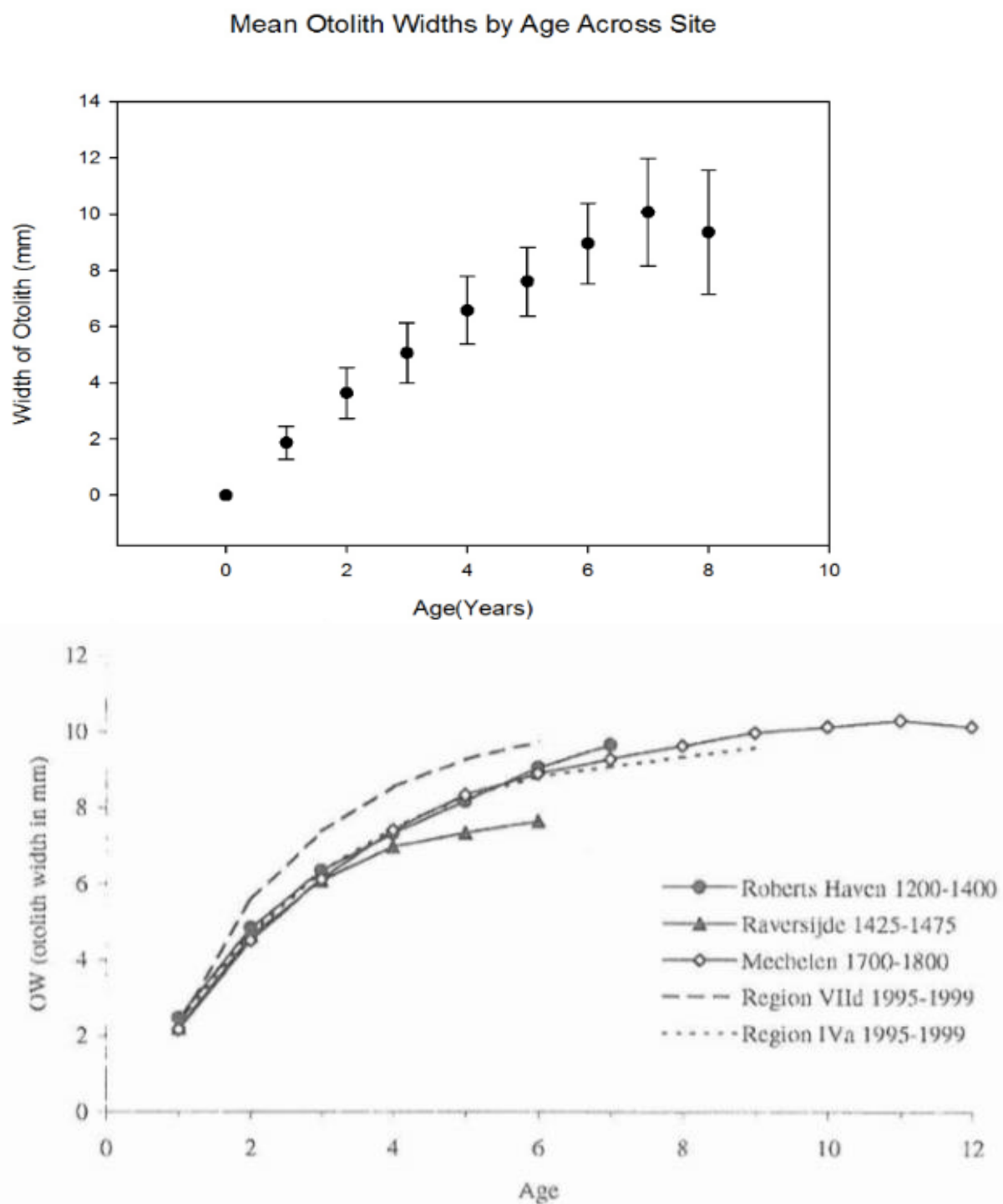


Figure 4.2 Our growth rate data(top) with growth rate data from Van Neer et al. 2002(bottom), 3 archaeological sites and 2 modern regions with average growth rate data from the Sandwich South site, region VIIId is immediately off the coast of the Netherlands, while region IVa is off the northwestern coast of Scotland

around Shetland is the relative strength of the Gulf Stream in comparison to the currents coming from the North Sea (Harwood et al. 2008). The Gulf Stream, which carries water from the tropics north, has a comparatively enriched $^{18}\text{O}/^{16}\text{O}$ signature (Figure 4.3). The North Sea, in comparison, is depleted in ^{18}O due to the influence of water coming from off of the European mainland as well as being an area of low evaporation (Figure 4.3). The major factor in determining the strength of the Gulf Stream relative to the currents from the North Sea is the North Atlantic Oscillation (Rimbu et al. 2003). Future work should be done on determining the effects of the North Atlantic Oscillation on the area around the Shetland Islands, as that would enable more certain paleoenvironmental reconstructions of the area.

Another source of error within this study is the lack of firm data on the seasonal bias present within otoliths in terms of their $^{18}\text{O}/^{16}\text{O}$ signature. Because most growth happens during the summer months, the resulting otolith would have more mass from summer months than winter months. Since fractionation is lower in warmer waters, this mass bias towards warmer months would impact the $^{18}\text{O}/^{16}\text{O}$ signature of the otolith, skewing the results of isotopic analysis towards warmer conditions and undervaluing the winter months. In other otolith studies, the methodology involves taking subsamples from the annuli in the otolith, avoiding the seasonal bias inherent in using whole otolith values (Hufthammer et al. 2010)

Due to evidence from the radiocarbon dates of a significant amount of exchange between the soils and otoliths at the Sandwick South site, the quality of the oxygen isotope data is suspect as well. Because ion exchange is unlikely to just affect a single carbon atom, but rather the carbonate ion that makes up half of aragonite, alterations to the ^{14}C of an otolith will also likely affect the $^{18}\text{O}/^{16}\text{O}$ ratio of the otolith. Because of this effect, any otoliths discarded due to suspected ionic exchange will not be analyzed for paleoclimate comparisons. This leaves 7

samples from which we have secure oxygen isotope data. However, most of these samples, like in the growth rate and fish length data, are from Midden Units 1 and 2, limiting the temporal scope to phase 2 of the occupation of the site. Within the otoliths that can be used, the average temperature is 9.54 degrees, slightly lower than the average if counting all the otoliths, but within the standard deviation. Modern sea surface temperatures for Shetland vary between 7.7°C in March and 13.3°C in August with the average modern annual temperature being 10.24°C (Sea Temperature 2017).

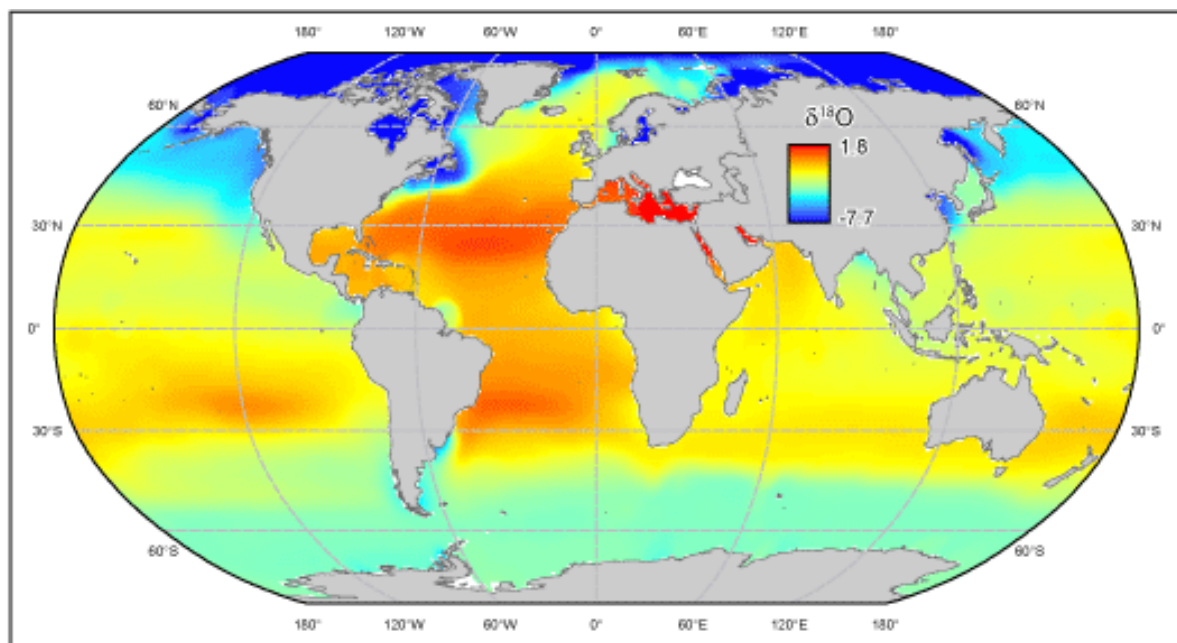


Figure 4.3 Isoscape from McMahon 2017 of ocean oxygen isotope values, with red representing more enriched and blue representing more depleted values. Note the yellow plume, the Gulf Stream, stretching up past England into the Arctic, and the dark blue fading to blue in the Baltic and North Seas

North Atlantic Paleotemperatures

Within the North Sea and northeastern Atlantic Ocean, there have been multiple studies done on ocean paleotemperatures done via sediment records. In Loch Sunart, western Scotland, temperature anomalies during the period of occupation were low in general, with a lone distinctive high and low pair of temperature anomalies happening around 1220 AD (Cage and

Austin 2010). While this pair of anomalies is not recorded in our data, those points are the exception to a generally stable period of time in the paleoceanographic record. This stability is also present in the Feni Drift, a sediment accumulation area of the western coast of Ireland (Richter et al. 2009). In the Richter et al. record, however, there is evidence of a slight cooling trend over the course of 1200-1350AD, which is not reflected clearly in our data.

In addition to ocean sediment derived studies, there have also been studies done on materials collected from peat bogs and lake sediments in England and Ireland. A study on sphagnum moss collected from a peat bog near Walton, England, found a relatively constant air temperature varying between 1 and 2 degrees above the mean temperature for the record during the period from roughly 900AD to 400AD, which would be consistent with the lack of trend found during phase 2 at the Sandwick South Site (Daley et al. 2010). Chironomid head capsule records collected by Langdon et al. from Talkin Tarn, Cumbria, England show a very different pattern, with a noticeable increase in temperature at the turn of the millennium followed by a decrease in water temperature at around 1400 AD (Langdon et al. 2004). While consistent with historical records of the beginning of the Little Ice Age, the increase in temperature is neither consistent with larger patterns of the Medieval Climatic Optimum, which peaked 200 years earlier, or with data from the Sandwick South Site, which does not show any marked increase or decrease in temperature over the period which we have data for.

In the larger North Atlantic context, there are records from the Greenland Ice Cap and the Skagerrak in the Baltic Sea that cover the period of occupation of the Sandwick South Site. The Greenland study finds a total increase in temperature from the occupation of the site to now of about 0.25°C to 0.5°C, which is less than the difference between modern Shetland sea surface temperatures and the calculated paleotemperatures, but that is attributable to the fact that cod live

lower in the water column than surface temperatures, resulting in a colder overall signature for the otoliths (Jansen et al. 2007). In the Skagerrak, $\delta^{18}\text{O}$ stability during the period of occupation was again the norm (Hass 1996). Both pairs of cores, in areas immediately northwest of Denmark, show similar signals in both species of foraminifera found in the cores. Within both pairs of cores, $\delta^{18}\text{O}$ variation during this period was less than $\pm 0.2\text{‰}$, showing only minor temperature variation in the Skagerrak during the occupation of the Sandwich South Site (Hass 1996).

Conclusions

Otolith ages

Radiocarbon dates from otoliths at the Sandwich South Site tend to skew older than the archaeological evidence suggests. Some samples have radiocarbon probability curves that overlap with archaeological evidence, but most do not. This is of note due to the implication of corruption of samples by ion exchange with the environment, which prevents accurate geochemical data from being gathered from many samples.

Fish Sizes

The range of fish sizes at the site suggest a standard Norse fishing colony, with both subsistence and trade fishing. While the distribution of fish sizes by otolith records is not bimodal, unlike previous studies done on fish remains at this site and many other Norse sites across the North Atlantic, the range is wider than many sites in the North Sea with only either trade or subsistence fish sizes. While taphonomic processes affected the sample preservation considerably, especially in regard to phases 1 and 3, within phase 2 sample preservation was high enough to provide insight into the economics of the site.

Growth Rates

The growth rates of the otoliths measured are not a good fit to previously defined cod growth rates but are within reasonable variation. Internal preservation of otoliths was poor due to a variety of

problems. Cod otolith annuli are difficult to see under microscope and lose definition towards the later years of the cod's life. In addition, staining from tannins in the soil dyed large portions of the otoliths so they were not readable. Thin sectioning of the otoliths was not done but would be a valuable addition to the research.

Paleoclimate Data

Within phase 2, our source for the majority of our samples, the reconstructed temperatures are similar to modern values, suggesting that sea temperatures during 1200-150 AD were similar to modern temperatures. These temperatures would be consistent with late Medieval Warm Period temperatures other places in the North Atlantic region (Langdon et al. 2004, Jansen et al. 2007, Daley et al. 2010). In phases 1 and 3, the stable isotope gathered was influenced by the ion exchange mentioned above, preventing any conclusions about paleotemperature over the entire occupation of the site.

Future Work

Future work at the site could focus on either the zooarchaeological side or the paleotemperature side of this study. For the size analysis, more samples could be measured, including those of other fish species collected at the site. These would help to expand the knowledge of the fishery characteristics of the site, enabling a more comprehensive picture of trade dynamics at the site and possible differences in fish use by species. Another avenue of further exploration would be making thin sections of the already cut otoliths. In thin section, otolith growth rings are significantly clearer, and more samples would be able to be accurately analyzed by this method, as well as increasing the accuracy of measurements made in this study.

The paleotemperature data could be further reinforced by other sources of firm dating, as one factor that hindered this study was the lack of definite dates within Phases 1 and 3. Also,

sources of $\delta^{18}\text{O}$ values other than otoliths would be extremely valuable, as most other oxygen containing materials at the site are more resistant to exchange with the environment, increasing their utility for both radiocarbon dating and $\delta^{18}\text{O}$ analysis. In addition, by subsampling different growth rings within the otolith, temperatures at different points in the cod's life could be calculated, giving a more accurate signal of temperatures at different positions in the water column as the cod ages.

References

- Amorosi, T., Buckland, P. C., Ólafsson, G., Sadler, J. P., and Skidmore P. 1992. *Site status and the palaeoecological record: a discussion of the results from Bessastaðir, Iceland*, pp. 169- 192. In *Norse and later settlement and subsistence in the North Atlantic*. Ed. by C. D. Morris and D. J. Rackham. Archetype Publications, University of Glasgow, Department of Archaeology.
- American Chemical Society, 2016, *Willard Libby and Radiocarbon Dating*, American Chemical Society website
- Barrett, J.H., 1997, *Fish trade in Norse Orkney and Caithness: A zooarchaeological approach*, *Antiquity*, Vol. 71, pp. 616-638
- Bigelow, G.F., 2017, Personal Communications, Bates College
- Bigelow, G.F., 1992, *Issues and Prospects in Shetland Norse Archaeology*, in Morris, C.D., Rackham, J., *Norse and Later Settlement and Subsistence in the North Atlantic*, University of Glasgow Department of Archaeology, Glasgow, UK, pp 3-15
- Bigelow G.F., 1989, *Life in Medieval Shetland: An archaeological perspective*, in Hikuin, F., Hikuin 15, Hikuin Moesgård, Denmark, pp. 183-191
- Bigelow, G.F., 1985, *Sandwick, Unst and Late Norse Shetland Economy*, in Smith, B., *Shetland Archaeology*, The Shetland Times Ltd, Lerwick, UK, pp.95-126
- Bradley, R.S., Hughes, M.K., Diaz, H.F., 2003, *Climate in Medieval Time*, *Science*, Vol 302, pp. 404-405
- Büntgen, U., Frank, D.C., Nievergelt, D., Esper, J., 2006, *Summer Temperature Variations in the European Alps, a.d. 755-2004*, *Journal of Climate*, Vol. 19

- Büntgen, U., Trouet, V., Frank, D., Leuschner, H.H., Friedrichs, D., Luterbacher, J., Esper, J.,
 2010, *Tree-ring indicators of German summer drought over the last millennium*,
 Quaternary Science Reviews, Vol. 29, pp. 1005-1016
- Bush, S.L., Santos, G.M., Xu, X., Southon, J.R., Thiagarajan, N., Hines, S.K., Adkins, J.F.,
 2013, *Simple, Rapid, and Cost Effective: a Screening Method for ^{14}C Analysis of Small
 Carbonate Samples*, University of Arizona
- Cage, A.G., Austin, W.E.N., 2010, *Marine Climate Variability during the last millennium: The
 Loch Sunart record*, Scotland, UK, Quaternary Science Reviews, Vol. 29, pp. 1633-1647
- Daley, T.J., Barber, K.E., Street-Perrott, F.A., Loader, N.J., Marshall, J.D., Crowley, S.F., 2010,
*Holocene climate variability revealed by oxygen isotope analysis of Sphagnum cellulose
 from Walton Moss, northern England*, Quaternary Science Reviews, Vol. 29, pp. 1590-
 1601
- Douka, K., Higham, T.F.G., Hedges, R.E.M., 2010, *Radiocarbon dating of shell carbonates: old
 problems and new solutions*, MUNIBE,
https://www.researchgate.net/publication/285978623_Radiocarbon_dating_of_shell_carbonates_old_problems_and_new_solutions/citations
- Eiríksson, J., Bára Bartels-Jónsdóttir, H., Cage, A.G., Gudmundsdóttir, E.R., Klitgaard-
 Kristensen, D., Marret, F., Rodrigues, T., Abrantes, F., Austin, W.E.N., Jiang, H.,
 Knudsen, K.-L., Sejrup, H.P., 2006, *Variability of the North Atlantic Current during the
 last 2000 years based on shelf bottom water and sea surface temperatures along an open
 ocean/shallow marine transect in western Europe*, The Holocene, 16 (7) (2006),
 pp. 1017-1029

- Hass, H.C., 1996, *Northern Europe climate variations during late Holocene: evidence from marine Skagerrak*, *Palaeogeography, Palaeoclimatology, Palaeoecology*, Vol. 123, 121-145
- Harwood, A.J.P., Dennis, P.F., Marca, A.D., Pilling, G.M., Millner, R.S., 2008, *The oxygen isotope composition of water masses within the North Sea*, *Estuarine, Coastal and Shelf Science*, Vol. 78, pp. 353-359
- Hoie, H., Otterlei, E., Folvord, A., 2004, *Temperature-dependent fractionation of stable oxygen isotopes in otoliths of juvenile cod (Gadus Morhua L.)*, *ICES Journal of Marine Science*, Vol. 61, No. 2, pp. 243-251
- Hufthammer, A.K., Hoie, H., Folkvord, A., Geffen, A.J., Andersson, C., Ninnemann, U.S., 2002, *Seasonality of human site occupation based on stable oxygen isotope ratios of cod otoliths*, *Journal of Archaeological Science*, vol 37, pp 78-83
- Jansen, E., J. Overpeck, K.R. Briffa, J.-C. Duplessy, F. Joos, V. Masson-Delmotte, D. Olago, B. Otto-Bliesner, W.R. Peltier, S. Rahmstorf, R. Ramesh, D. Raynaud, D. Rind, O. Solomina, R. Villalba and D. Zhang, 2007: *Palaeoclimate. In: Climate Change 2007: The Physical Science Basis*. Contribution of Working Group I to the Fourth Assessment Report of the Intergovernmental Panel on Climate Change [Solomon, S., D. Qin, M. Manning, Z. Chen, M. Marquis, K.B. Averyt, M. Tignor and H.L. Miller (eds.)]. Cambridge University Press, Cambridge, United Kingdom and New York, NY, USA.
- Krivogorskaya, Y., Perdikaris, S., McGovern, T.H., 2005, *Fish bones and Fishermen: the potential of Zooarchaeology in the Westfjords*, *Archaeologica Islandica*, Vol. 4, pp. 31-51
- Lamb, H.H., 1982, *Climate, History and the Modern World*, Routledge, New York, New York

- Langdon, P.G., Barber, K.E., Lomas-Clarke, S.H., 2004, *Reconstructing climate and environmental change in northern England through chironomid and pollen analyses: evidence from Talkin Tarn, Cumbria*, Journal of Paleolimnology, Vol. 32, pp. 197-213
- LeGrande, A.N., Schmidt, G.A., 2006: *Global gridded data set of the oxygen isotopic composition in seawater*. Geophys. Res. Lett., **33**, L12604, doi:10.1029/2006GL026011.
- Mann, M.E., Zhang, Z., Rutherford, S., Bradley, R.S., Hughes, M.K., Shindell, D., Ammann, C., Faluvegi, G., Ni, F., 2009, *Global Signatures and Dynamical Origins of the Little Ice Age and Medieval Climate Anomaly*, Science Magazine, Vol 326, pp. 1256-1260
- McMahon, K., 2017, *Ocean Isoscapes*, UCSC
- Richter, T.O., Peeters, F.J.C., van Weering, T.C.E., 2009, *Late Holocene (0–2.4 ka BP) surface water temperature and salinity variability, Feni Drift, NE Atlantic Ocean*, Quaternary Science Reviews, 28 (19–20) (2009), pp. 1941-1955
- Schmidt, G.A., G. R. Bigg and E. J. Rohling. 1999. "Global Seawater Oxygen-18 Database - v1.22" <https://data.giss.nasa.gov/o18data/>
- Seatemperature.org, 2017, *Shetland Sea Temperature*,
<https://www.seatemperature.org/europe/united-kingdom/shetland.html>
- Sharp, Z., 2017, Principles of Stable Isotope Geochemistry, University of New Mexico, chapter 5.2
- Surge, D., Barret, J.H., 2012, *Marine climatic seasonality during medieval times (10th to 12th centuries) based on isotopic records in Viking Age shells from Orkney, Scotland*, Paleogeography, Paleoclimatology, Paleoecology, vol. 350-352

Stable Isotope Paleo-Environments Research Group, 2017, Stable Isotope Lab, Iowa State University

Stuiver, M., Reimer, P.J., and Reimer, R.W., 2017, CALIB 7.1 [WWW program] at <http://calib.org>, accessed 2017-11- 25

Van Neer, W., Ervynck, A., Bolle, L.J., Millner, R.S., Rijnsdorp, A.D., 2002, *Fish Otoliths and their relevance to Archaeology: An Analysis of Medieval, Post-Medieval, and Recent Material of Plaice, Cod and Haddock from the North Sea*, Environmental Archaeology, Vol. 7, pp. 61-76